Teknillinen korkeakoulu. Konetekniikan osasto. LVI-tekniikan laboratorio. A
Helsinki University of Technology. Department of Mechanical Engineering.
Laboratory of Heating, Ventilating and Air Conditioning. A
Espoo 2003

MATHEMATICAL MODELLING AND EXPERIMENTAL INVESTIGATION OF MELTING AND SOLIDIFICATION IN A FINNED PHASE CHANGE MATERIAL STORAGE

REPORT A8

Piia Lamberg

Teknillinen korkeakoulu. Konetekniikan osasto. LVI-tekniikan laboratorio. A
Helsinki University of Technology. Department of Mechanical Engineering.
Laboratory of Heating, Ventilating and Air Conditioning. A
Espoo 2003

MATHEMATICAL MODELLING AND EXPERIMENTAL INVESTIGATION OF MELTING AND SOLIDIFICATION IN A FINNED PHASE CHANGE MATERIAL STORAGE

REPORT A8

Piia Lamberg

Dissertation for the degree of Doctor of Science in Technology to be presented with due permission of the Department of Mechanical Engineering, Helsinki University of Technology for public examination and debate in Auditorium K216 at Helsinki University of Technology (Espoo, Finland) on the 5th of December, 2003, at 12 noon.

Helsinki University of Technology
Department of Mechanical Engineering
Laboratory of Heating, Ventilating and Air Conditioning

Distribution:

Helsinki University of Technology
HVAC-Library
P.O. Box 4100
FIN-02015 HUT
Tel. +358 9 451 3601
Fax. +358 9 451 3611

Author's address:
Insinööritoimisto Olof Granlund Oy
P.O.Box 41
FIN-00701 Helsinki
Tel.+358 9 4510 3387
Fax.+358 9 4510 3424
E-mail: piia.lamberg @granlund.fi

Supervisor:
Professor Kai Siren
Helsinki University of Technology

Reviewers:
Professor Vasilios Alexiades
The University of Tennessee, Knoxville

Professor Antero Aittomäki
Tampere University of Technology

Opponents:
Professor Björn Palm
Royal Institute of Technology, Sweden

Professor Antero Aittomäki
Tampere University of Technology

ISBN 951-22-6608-3 (PDF format)
ISBN 951-22-6607-5
ISSN 1238-8971

Otamedia Oy
2003

ABSTRACT

In latent heat storage, internal heat transfer enhancement techniques such as fins have to be used because of the low heat conductivity of the phase change material (PCM). During the phase change in a PCM storage system the solid-liquid interface moves away from the heat transfer surface and the surface heat flux decreases due to the increasing thermal resistance of the molten or solidified medium. Internal heat transfer enhancement is essential, especially in a solidification process where the main heat transfer mode is conduction.

The objective of this study was to develop an analytical model which predicts the solid-liquid interface location and temperature distribution of the fin in melting and especially, in solidification processes with a constant end wall temperature in a finned two-dimensional PCM storage. Heat transfer during the melting and solidification processes in a finned PCM storage was also studied numerically and experimentally. The objective of the experimental work was to evaluate different numerical methods in order to find a reliable numerical method for the comparison of several PCM storage structures.

The results of the derived analytical model were compared to numerical results calculated with the FEMLAB multiphysics simulation tool and Digital Fortran 5.0. The simplified analytical equations were solved with FEMLAB in order to find out the accuracy of the analytical solution. The two-dimensional heat transfer problem was also solved numerically by means of the effective heat capacity method and enthalpy method, using FEMLAB and Digital Fortran. The two-dimensional results were compared to simplified one-dimensional results in order to find out the accuracy of the simplified analytical model. The results of the experimental work were compared to the numerical results calculated with FEMLAB, using the effective heat capacity method and enthalpy method, in order to find out the accuracy of different numerical methods.

A simplified analytical model based on a linear, transient, thin-fin equation was introduced which predicts the solid-liquid interface location and temperature distribution of the fin in the melting process with a constant imposed end wall temperature for the melting process in a semi-infinite PCM storage and for the solidification process in a finite PCM storage with internal fins. The results show that the analytical models give a satisfactory estimate of fin temperature and the solid-liquid interface. It was noticed that the assumptions made in simplifying the two-dimensional heat transfer problem into a one-dimensional form affected the accuracy to a greater extent than the assumptions made when solving the one-dimensional equations analytically.

The results showed that the effective heat capacity method with a narrow temperature range, dT=2°C, was the most precise numerical method when numerical results were compared to experimental results in a finned paraffin PCM storage. The FEMLAB program was very suitable for solving different kinds of phase change problems in one, two, or three dimensions.

PREFACE

The work presented in the thesis was carried out mainly at the Laboratory of Heating, Ventilating, and Air Conditioning of Helsinki University of Technology during the years 1998-2001, when I was in Graduate school of Building Physics. The Graduate School was funded by the Academy of Finland, who are gratefully acknowledged for sponsoring this work. The work was finished while I was working in the private sector, at Olof Granlund Oy. The financial support provided by L.V.Y säätiö, K.V. Lindholm Stiftelsen and Koskenniemi säätiö, as well as Olof Granlund Oy for supporting language checking, are also gratefully acknowledged.

I wish to thank my supervisor, Prof. Kai Siren, for his continuous support, encouragement, and valuable advice during the course of my work.

I would also like to thank my co-authors, Reijo Lehtiniemi, Ph.D, and Anna-Maria Henell, M.Sc, from the Nokia Research Centre, for their interesting and fruitful co-operation during the research work. Special thanks are also expressed to Jari Pennanen, Ph.D, from Comsol Oy for his valuable support and assistance with the numerical calculations.

Finally, many thanks to my family and friends for their support during these seemingly endless years of studies and for putting up with my ups and downs. The greatest thanks are expressed to my dear fiancé Petri. It took n+2 years, but now it is finally ready. Thank you for being there for me.

I wish to dedicate this work to the three men in my life: my fiancé Petri, my brother Ville, and my father Markku.

Vantaa, June 2003

Piia Lamberg

TABLE OF CONTENTS

LIST OF PUBLICATIONS

I. Lamberg P, Lehtiniemi R, Henell A.-M., Numerical and experimental investigation of melting and freezing processes in phase change material storage. Accepted for printing in International Journal of Thermal Sciences, July 2003.

II. Lehtiniemi R, Lamberg P, Henell A.-M., Validating a numerical phase change model by using infrared thermography. Proceedings of the 6th International Conference on Quantitative Infrared Thermography, QIRT 2002, Dubrovnik, September 24-27, 2002.

III. Lamberg P, Siren K, Analytical model for melting in a semi-infinite PCM storage with an internal fin. Heat and Mass Transfer, Vol. 39, pp. 167-176, 2003.

IV. Lamberg P, Siren K, Approximate analytical model for solidification in a finite PCM storage with internal fins. Applied Mathematical Modelling, Vol 27/7, pp. 491-513, 2003.

V. Lamberg P, Approximate analytical model for two-phase solidification problem in a finned phase change material storage. Applied Energy, Vol. 77, pp. 131-152.

The author is the principal author of four of these publications (I, III-V). In Publication II the author was responsible for carrying out the numerical analysis of the heat transfer problem in finned phase change material storages. The experimental work was the responsibility of my co-authors, Reijo Lehtiniemi, Ph.D, and Anna-Maria Henell, M.Sc. The analysis of the results and conclusions was performed together.

NOMENCLATURE

c_p	heat capacity, J kg^{-1}K^{-1}
D	half-thickness of the fin, height of the storage, m
Eff_2	effective heat capacity method (dT=2°C)
Eff_7	effective heat capacity method (dT=7°C)
Ent	enthalpy method
Exp	experimental
H	total enthalpy, J
h	convection heat transfer coefficient, W m^{-2}K^{-1}
k	heat conductivity, W m^{-1}K^{-1}
l	length, m
l_c	height of the storage, m
l_f	length of the fin, m
L	latent heat of fusion, J kg^{-1}
$\bar{n}$	the normal of the solid-liquid interface
Ra	Rayleigh number, $Ra = \frac{g\beta\Delta TL^3}{\alpha\nu}$, -
S	location of the phase change interface, m
St	Stefan number, $St = \frac{c_p\Delta T}{L}$, -
T	temperature, °C
dT	melting or solidification temperature range, °C
ΔT	temperature difference, °C
t	time, s
x	distance in the x-direction, m
y	distance in the y-direction, m

Greek symbols

α	thermal diffusivity, m^{2}s^{-1}
ρ	density, kg m^{-3}
ε	fraction of solidified PCM
λ	root of the transcendental equation
$\bar{v}$	velocity of the PCM, m s^{-1}
μ	dynamic viscosity, kg m^{-1}s^{-1}
$\theta = \frac{T-T_m}{T_w-T_m}$	dimensionless temperature distribution
$\tau = \frac{k_f t}{(\rho c_p)_f l_f^2}$	dimensionless time
$\gamma = \frac{S_y}{l_c}$	dimensionless rate of solid-liquid interface recession

$\eta = \frac{x}{l_f}$ dimensionless x-coordinate

$\lambda = \frac{l_f}{l_c}$ cell aspect ratio

$\Psi = \frac{D}{l_c}$ dimensionless half-thickness of the fin

$\kappa = \frac{k_s}{k_f}$ ratio of the heat conductivities

$\xi = \frac{(\rho c_p)_f (T_w - T_m)}{-L\rho_s}$ modified Stefan number

Subscripts

c	convection, cell
f	fin
i	initial
l	liquid
m	melting or solidification
n	normal
eff	effective
p	phase change material
s	solid
w	wall
x	x-direction
y	y-direction

1 INTRODUCTION

1.1 Background

Phase change material (PCM) storages are used to balance temporary temperature alternations and store energy in several practical application areas, from food and vaccine transportation to electronics, the automobile industry, and buildings. When a temperature peak of the heat transfer medium or the surroundings of the storage occurs, the PCM absorbs the excess energy by going through a phase transition and then releases the absorbed energy later, when the peak has passed. For example, in contemporary telecommunications electronics, both portable and larger-scale, thermal transitions due to temporary variations in power dissipation are customary. The use of PCM storages to compensate for the temperature peaks that occur may offer a remarkable difference in the time-dependent thermal management of the products.

The PCMs most commonly used in storing energy are paraffins, salt hydrates, and fatty acids. These materials exhibit significant latent heat of fusion behaviour during phase change. However, the materials also have some disadvantages, such as weak stability, a lack of durability, and supercooling effects. The crystallising and thickening agents which are used to prevent supercooling and phase separation in the PCM lower the thermal conductivity of the PCM and the inhibiting convection motion in the liquid PCM (Padmahabhan et al. 1986; Veljar et al. 1999). The heat conductivity of paraffins varies between 0.1-0.2 W m-1K-1 and that of salt hydrates between 0.4-0.6 W m-1K-1, depending on the material (Peippo 1989). During the phase change the solid-liquid interface moves away from the heat transfer surface. At the same time heat flux decreases due to the increasing resistance of the growing layer of molten or solidified PCM. Internal heat transfer in PCM storages can be enhanced with fins, metal honeycombs, metal matrices (wire mesh), rings, high-conductivity particles, or graphite (Kroeger et al. 1973; Mehling 2000).

This work concentrates on the heat transfer enhancement of storages with internal fins. Consider the PCM storage shown in Fig. 1. The PCM storage consists of a metallic housing in the shape of a parallelepiped. The storage is filled with PCM and straight metal fins which improve heat transfer between the housing and the phase change material. The two end walls are affected by the temperature change. The other two walls are assumed to be insulated.

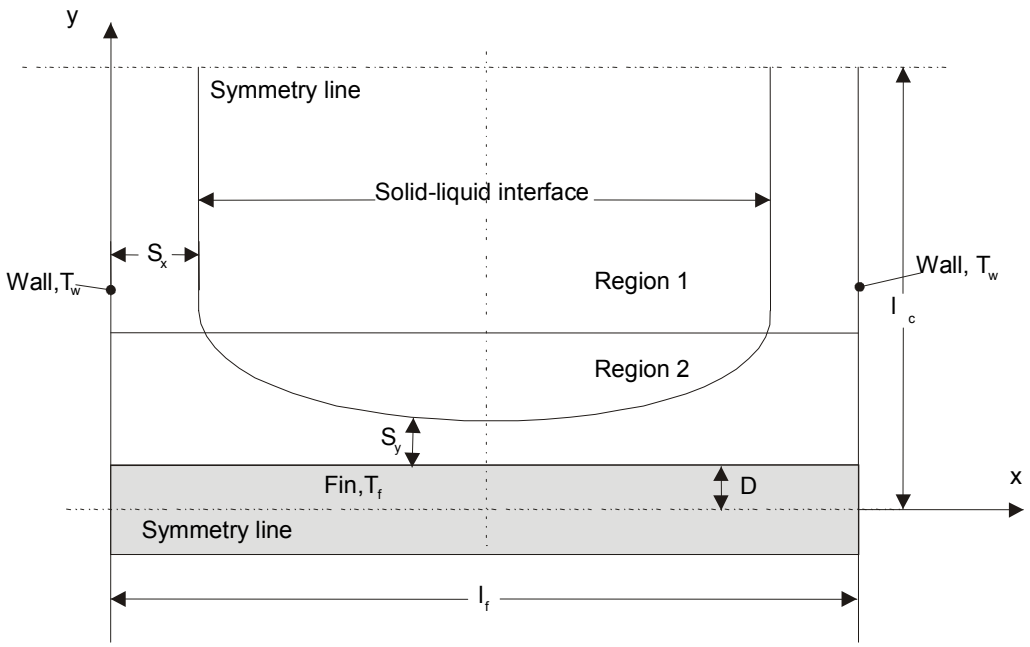

Figure 1. The finned PCM storage.

In the melting process PCM is initially in a solid state at a lower temperature than, or the same temperature as, its melting temperature. The material starts to melt and store energy when the end walls are exposed to a higher temperature than the melting temperature of the PCM. On the other hand, in the solidification process PCM is initially at a higher temperature than, or the same temperature as, its solidification temperature. The material starts to solidify when the walls are exposed to a lower temperature than the solidification temperature of the material.

In the melting process, heat is transferred from the walls, first by conduction through the fin and the PCM, and later by natural convection through the PCM. Natural convection accelerates the melting process. In the solidification process, heat is transferred by conduction along the fins and through the solidified phase change material from the solid-liquid interface to the end walls. Natural convection exists in the liquid-solid interface due to the temperature difference in the liquid PCM. But even very strong natural convection in the solid-liquid interface has a negligible effect on the solid-liquid interface position compared to the effect of heat conduction in solid PCM (Kroeger et al. 1973). The solidification process is much slower than the melting process because natural convection does not speed up solidification.

The governing equations for transient analyses of the melting of the phase change material includes the Navier-Stokes (momentum) equations, the continuity equation, and the energy equation. The Boussinesq approximation is used to model the buoyancy forces. The equations are the following, given in tensor notation:

$$\rho \frac{\partial \vec{v}}{\partial t} + \rho(\vec{v} \bullet \nabla)\vec{v} = -\nabla p + \mu \nabla^2 \vec{v} + \rho \vec{g}\,\beta(T - T_o) \qquad (1)$$

$$\nabla \bullet \vec{v} = 0 \tag{2}$$

$$\rho_l c_{pl}\left(\frac{\partial T_l}{\partial t} + \nabla \bullet (\vec{v} T_l)\right) = \nabla \bullet (k_l \nabla T_l) \tag{3}$$

where ρ_l is the density, $\bar{v}$ the velocity of the liquid PCM, p the pressure, μ the dynamic viscosity, g the gravity vector, β the coefficient of thermal expansion, T_o the reference temperature, c_l the specific heat, k_l the heat conductivity and T_l the temperature of the liquid PCM.

For the solid PCM and the enclosure the Eqs.(1) and (2) can be ignored because there is no convection effect on the materials. The energy equation is given the form

$$\rho_s c_s\left(\frac{\partial T_s}{\partial t}\right) = \nabla(k_s \nabla T_s) \tag{4}$$

where the subscript s denotes the solid PCM.

In the solid-liquid interface the net amount of heat, which achieves the solid-liquid interface in a time unit, moves the distance of the phase change interface, which depends on the latent heat of the material. When density of the solid and liquid material is equal and the convection heat transfer is ignored in the liquid PCM, the energy balance for the solid-liquid interface in the melting process takes the form (Lane 1983):

$$k_s \left.\frac{\partial T_s}{\partial \bar{n}}\right|_S - k_l \left.\frac{\partial T_s}{\partial \bar{n}}\right|_S = \rho_s L \frac{dS_n}{dt} \tag{5}$$

where S is the solid-liquid phase change interface, n the normal of the solid-liquid interface, and L the latent heat of fusion of the PCM. In the solidification process the subscripts l and s are interchanged and the latent heat of fusion L is replaced with $-L$ in Eq.(5).

If the natural convection in the liquid PCM is taken into account the energy balance for the solid-liquid interface is

$$k_s \left.\frac{\partial T_s}{\partial \bar{n}}\right|_S + h\Delta T_n = \rho_s L \frac{dS_n}{dt} \tag{6}$$

where h is the convection heat transfer coefficient in the solid-liquid interface and ΔT_n is the temperature difference between solid-liquid interface and the boundary in the normal direction of the solid-liquid interface.

Heat transfer in a PCM storage is a transient, non-linear (Eqs. (1)-(6)) phenomenon with a moving solid-liquid interface, generally referred to as a "moving boundary" problem. Non-linearity is the source of the difficulties when solving mathematically moving boundary problems. Therefore, the analytical solution of the phase change problems is known only for a couple of physical situations with simple geometry and boundary conditions. Thus, an analytical solution for the heat transfer problem in finned PCM has not been found. However, heat transfer in phase change material with internal fins has been studied numerically and experimentally over a wide range. The most commonly used numerical methods in the literature have been the enthalpy method and the effective heat capacity method (Crank 1984; Bonacina 1973; Alexiades et al. 1993).

Velraj et al. (1997, 1999) studied experimentally and numerically different heat transfer enhancement techniques for a solar thermal storage system focusing on fins, rings, and air bubbles, and performed experimental and numerical studies of inward solidification on a finned vertical tube for a latent heat storage unit. The results showed that the solidification time in a finned tube was reduced by a factor of approximately 1/n (where n is the number of fins in the tube) compared to the case without fins.

Al-Jandal (1992) studied experimentally what effects the fin, metal honeycomb, and copper matrix structure have on the total melting and solidification time. The results showed that the average thermal conductivity enhancement factors for solidification were of the order of 1.7 and those for melting of the order of 3.3. Natural convection had a significant effect on the acceleration of melting. The average thermal conductivity enhancement factor was determined as a ratio of solidification or melting time with fins and without fins.

Stritih et al. (2000) handled heat transfer enhancement in the solidification process in a finned PCM storage with a heat exchanger both numerically and experimentally. Their conclusion was that the greatest influence on heat transfer in the solidification process was the distance between the fins. The thickness of the fins was not as influential.

Humpries et al. (1977) studied a rectangular phase change housing numerically, using straight fins as a heat transfer enhancer in a 2-dimensional grid. The data were generated over a range of realistic sizes, material properties, and different kinds of thermal boundary conditions. This resulted in a design handbook for phase change energy storages.

Bugaje (1977) made experiments on the use of methods for enhancing the thermal response of paraffin wax heat storage tubes with the incorporation of aluminium fins and star structures. The conclusion was that internal fins performed much better than star matrices, reducing the loading time by a magnitude of 2.2 and the cooling time by a magnitude of 4.2.

A simplified numerical model based on a linear, transient, thin-fin equation which predicts the fraction of melted PCM and the shape of the liquid-solid interface as a function of time in a finite storage was introduced by Henze et al. (1981). Experimental

results were compared in dimensionless form with model predictions and showed fairly good agreement. To achieve high heat transfer rates with a fixed amount of PCM and metal fin material, the model indicated that melting the PCM in a pure conduction mode with closely-spaced thin fins was preferable to melting PCM with thicker fins spread further apart, even in the presence of natural convection.

The emphasis in the literature has been mainly on studying what effects the fins have on the melting and solidification speed in a finned PCM storage. However, the numerical and experimental methods used in the studies are complicated and time-consuming. In everyday engineering work there is often no opportunity to concentrate on complicated numerical computations or experimental work during the predesign of a storage. A fast analytical model would save time and effort. Design tools which are based on analytical models require less computational power and are easier to use. An effective simulation tool for numerical calculations in a finned PCM storage and the accuracy of the different numerical methods also need to be tested for the purpose of everyday engineering work.

1.2 Objective and content of the study

The objective of this study was to develop an analytical model which predicts the solid-liquid interface location and temperature distribution of the fin in the melting and, especially, solidification processes with a constant end wall temperature in a finned two-dimensional PCM storage. Heat transfer in a finned PCM storage was also studied experimentally and numerically with the FEMLAB multiphysics simulation tool.

The special objectives for the research were the following:

- to study the accuracy of the numerical methods (enthalpy method and effective heat capacity method) by comparing the numerical results to experimental results;
- to study the suitability of the FEMLAB multiphysics simulation tool for numerical calculations in phase change heat transfer problems;
- to test the feasibility of using an infra-red (IR) camera to perform fast, quantitative visualisation of the test case during the experimental work;
- to develop an analytical model for the melting process in a semi-infinite PCM storage with constant temperature boundary conditions. The PCM is initially at the solidification temperature of the PCM;
- to develop an analytical model for the solidification process in a finite PCM storage with constant temperature boundary conditions. The PCM is initially at the solidification temperature of the PCM, and
- to develop an analytical model for the solidification process in a finite PCM storage with constant temperature boundary conditions. The initial temperature of the PCM is higher than its solidification temperature.

The thesis consists of five papers. In Papers I and II different numerical methods were employed in an endeavour to discover a straightforward and reliable method for quick parametric studies and the comparison of several PCM storage alternatives. The

numerical methods studied were the enthalpy method and effective heat capacity method. PCM storages, with and without heat transfer enhancement structures, were designed and constructed. The numerical predictions calculated with the FEMLAB multiphysics program were compared to experimental data. Additionally, the feasibility of using an IR camera to perform fast, quantitative visualisation of the test case was tested. Both numerical methods gave a good estimate of the temperature distribution of the storages during the melting and freezing processes. However, the effective heat capacity method with a narrow temperature range, dT=2°C, was the most precise numerical method when numerical results were compared to experimental results. It was also noticed that the thermocouple recordings for the temperature of the storage were more reliable than the results achieved with an IR camera.

In Paper III a simplified analytical model based on a linear, transient, thin-fin equation which predicts the solid-liquid interface location and temperature distribution of the fin in the melting process in a semi-infinite PCM storage with internal fins was presented. The end wall temperature was considered to be constant in the model and the storage was assumed to be at the solidification temperature of the PCM. The two-dimensional heat transfer problem was simplified into a one-dimensional problem. The equations were solved mathematically and an analytical solution for the problem was presented. The analytical results were compared to the numerical results and they showed good agreement. Due to the assumptions made in the analytical model, the speed of the solid-liquid interface during the melting process was slightly too slow in the analytical results when compared to the numerical results.

The work done in Paper III was extended in Paper IV to consider the solidification process. A simplified one-dimensional analytical model which predicted the solid-liquid interface location and temperature distribution of the fin in the solidification process with a constant end wall temperature in a finned two-dimensional PCM storage was presented. The storage was assumed to be initially at the solidification temperature of the PCM. The heat transfer in the PCM storage was also calculated with a simplified one-dimensional numerical model and a two-dimensional numerical model. By comparing the results of different methods it was possible to draw conclusions regarding the accuracy of the simplified one-dimensional analytical model. A factor, called the fraction of solidified PCM, was also introduced in the paper. The results showed that the assumptions made in simplifying the two-dimensional heat transfer problem into a one-dimensional form affected the accuracy to a greater extent than the assumptions made when solving the one-dimensional equations analytically. However, the accuracy of the derived analytical model was good.

In Paper V the analytical approach to the solidification process was extended to cover the case where the storage was initially in a liquid state and its temperature was higher than the solidification temperature of the PCM. The analytical results were compared to the numerical results calculated by using the heat capacity method. The results showed that the analytical model gave a satisfactory estimation for the fin temperature and the solid-liquid interface when the length-to-height ratio of the storage cell (λ) is smaller than 6.0 and the fin length is smaller than 0.06 m. The error made in the fraction of

solidified PCM is ±10% when the analytical model was used rather than the two-dimensional numerical model.

An analytical solution for the heat transfer problem in finned two-dimensional PCM storage has not been found from the literature. In this work an analytical model which predicts the solid-liquid interface location and temperature distribution of the fin in melting and especially, in solidification processes with a constant end wall temperature in a finned two-dimensional PCM storage was presented for the first time. Heat transfer during the melting and solidification processes in a finned PCM storage was also studied numerically and experimentally. Different numerical methods were evaluated and a reliable numerical method for the comparison of several PCM storage structures was found.

2 NUMERICAL AND EXPERIMENTAL INVESTIGATION OF MELTING AND FREEZING PROCESSES IN PCM STORAGES

In Papers I and II, heat transfer in a small PCM storage was studied numerically and experimentally. The aim of the study was to evaluate different numerical methods in order to find a straightforward and reliable numerical method for quick parametric studies and the comparison of several PCM storage alternatives. The numerical methods studied were the enthalpy method and effective heat capacity method. An ensemble of experimental PCM storages, with and without heat transfer enhancement structures, was designed and constructed. The numerical predictions calculated with the FEMLAB multiphysics simulation tool were compared to experimental data. Additionally, the feasibility of using an IR camera to perform fast, quantitative visualisation of the test case under study was tested.

2.1 Experiments

The phase change material used in the experiments was technical grade paraffin. To find out the behaviour of the PCM during the melting and freezing process the DSC measurements were performed with Mettler TA4000 thermoanalysis equipment with a liquid nitrogen cooling system. From the measurements, it was possible to determine the latent heat of fusion in the melting and solidification processes. The DSC-curve for the melting and freezing processes of the paraffin is shown in Fig.2.

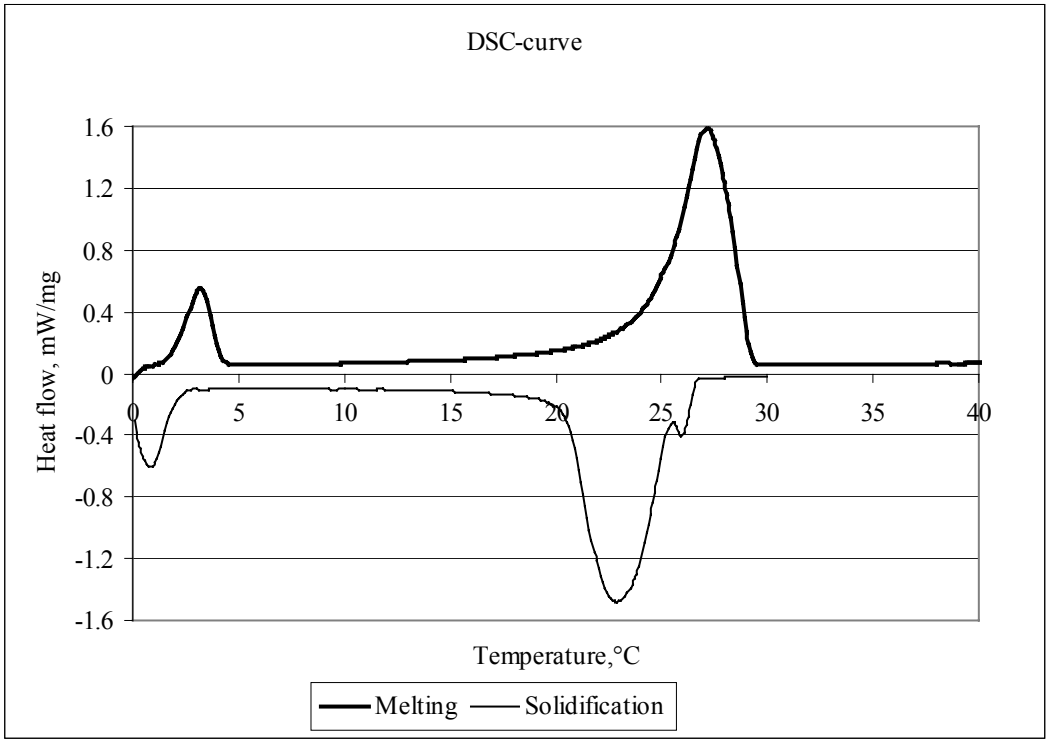

Figure 2. The DSC-curve of the paraffin.

The material starts melting when it achieves a temperature of 20-21°C. The peak temperature of the melting is 27.7°C. At the peak temperature the material stores or releases the greatest amount of energy. Solidification starts when the material achieves a temperature of 26.5°C and the peak temperature of the solidification is 23°C. The latent heat energy is released completely when the temperature of the material approaches 21°C.

The material properties of the material are presented in Table 1.

Table 1. The material properties of technical grade paraffin.

	paraffin
Density solid/liquid 15/70°C (ρ) kg m^{-3}	789 / 750
Heat conductivity solid/liquid (k) Wm^{-1}K^{-1}	0.18 / 0.19
Heat capacity solid / liquid (c_p) kJkg^{-1}K^{-1}	1.8 / 2.4
Volume expansion at ΔT=20°C, %	4.9
Heat storage capacity ΔH, melting ΔT=10->40°C, Jkg^{-1}	175066
Heat storage capacity ΔH, solidification ΔT=40->10°C, Jkg^{-1}	187698

The heat storage capacity of the material differs during melting and freezing processes because of measurement errors during DSC- measurements and calculation method used. In theory the heat capacity of the material is equal during melting and freezing processes.

Two different kinds of PCM storage were manufactured, one simple container (Storage 1, Fig. 3a) and one equipped with internal fins which enhance heat transfer inside the storage (Storage 2, Fig. 3b).

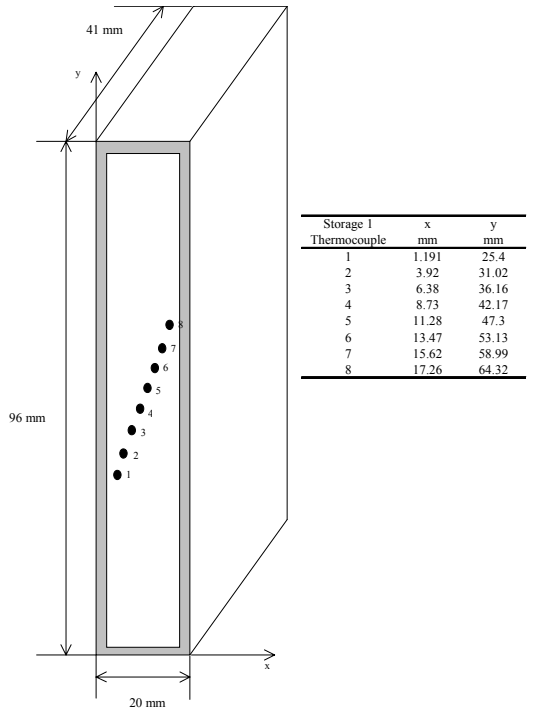

Storage 1 Thermocouple	x mm	y mm
1	1.191	25.4
2	3.92	31.02
3	6.38	36.16
4	8.73	42.17
5	11.28	47.3
6	13.47	53.13
7	15.62	58.99
8	17.26	64.32

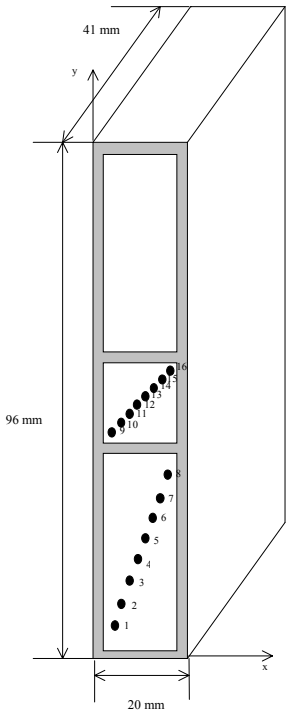

Storage 2 Thermocouple	x mm	y mm
1	2.238	8.123
2	4.598	11.185
3	6.382	14.16
4	8.577	18.16
5	11.312	21.261
6	13.663	23.961
7	15.579	27.75
8	17.12	31.844
9	1.956	40.238
10	4.599	41.731
11	6.536	44.198
12	8.565	46.391
13	9.693	48.342
14	12.078	51.444
15	14.629	53.647
16	16.531	55.821

Figure 3. PCM storages: a) without fins, Storage 1; b) with fins, Storage 2. The depth of the storage in the z-direction is 41 mm.

The heat storages used for the measurements were fabricated from solid aluminium blocks by machining the interior away by means of the electro-discharge method to ensure flawless heat transfer in the aluminium without any additional contact resistances due to joints. The storages were equipped with K-type thermocouples, which were arranged as shown in Figs. 3a and 3b. The supports were fabricated of FR4 epoxy-glass fibre composite.

For the IR measurements, the emissivity of paraffin was determined experimentally by calibrating the IR camera against known temperatures both in solid and in liquid phase paraffin. A ZnSe infrared window with 70% transmission at the IR camera operating wavelength range was mounted as the lid of the PCM storage using nitrile rubber sealing and phenolic fabric window support. The measurement set-up is shown schematically in Fig. 4. An FLIR SC3000 Quantum Well IR Photodetector (QWIP) camera was mounted so that it had a direct view of the PCM surface inside the storage behind the ZnSe IR window. The window is placed z=0. The camera operated at an 8-9 μm wavelength and was equipped with three lenses: standard optics (20° x 15°, 1.1 mrad IFOV); one close-up lens with a 34 mm x 26 mm imaging area, and one with a 10

mm x 7.5 mm imaging area. The thermal sensitivity of the camera at room temperature was less than 20 mK and its measurement accuracy better than ±1% or ±1°C, whichever was larger. With the camera, it was possible to record a 320 x 240-pixel live thermal image at a 50 Hz frame rate.

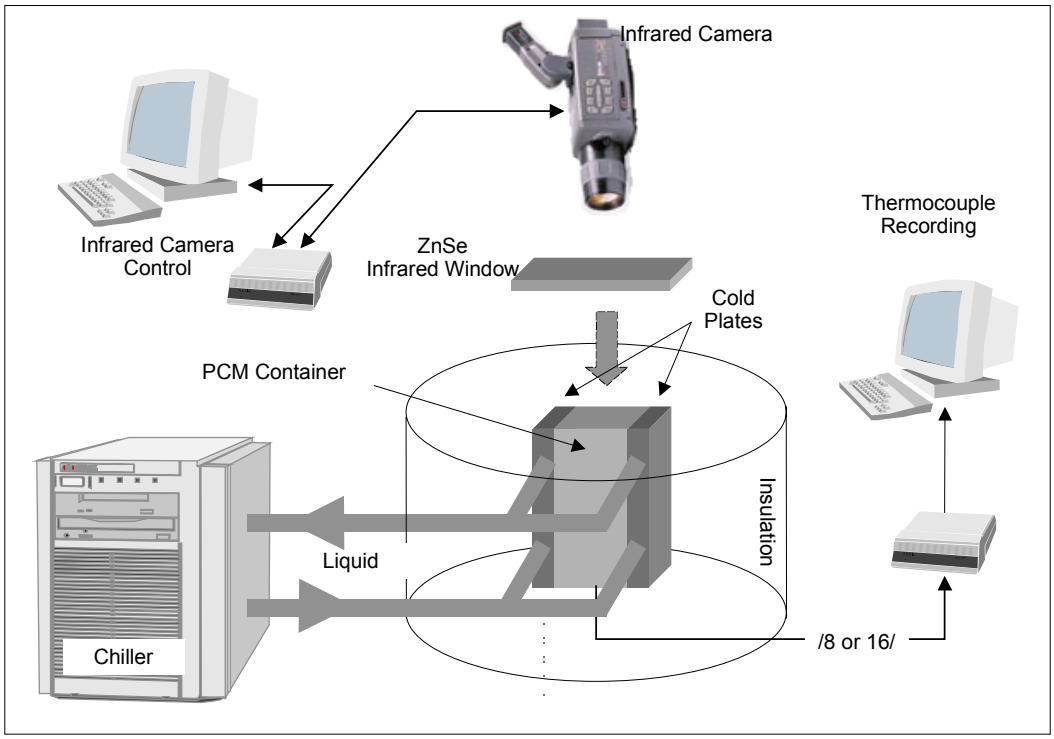

Figure 4. The measurement set-up.

Two identical aluminium cold plates with an coolant current of 4 l/min were mounted on opposite sides of the container at x=0 mm and x=20 mm. The cold plates and the remaining walls of the storage were isolated from the environment with Styrofoam. The heat transfer medium used in the experiments was water.

In the measurements, the liquid circulation chiller was first set to cool the cold plates to +10°C. When the steady state temperature was reached, the cooling water temperature was set to +40°C and the system was allowed to develop towards the new equilibrium. After all the PCM had melted and the system was in a +40°C steady state condition, the cooling water temperature was set back to +10°C. The entire 10°C-40°C-10°C cycle took about 2.5–3 hours and it was repeated at least five times for each measurement case. For each cycle, the temperature responses of either eight (Storage 1) or 16 (Storage 2) thermocouples and thermal images of the PCM surface were recorded at one-minute intervals.

2.2 Numerical methods

The most commonly used numerical methods in modelling heat transfer problems in PCM are the enthalpy method and the heat capacity method. In reality, in phase change situations more than one phase change interface may occur or the interfaces may disappear totally. Furthermore, the phase change usually happens in a non-isothermal temperature range. In such cases tracking the solid-liquid interface may be difficult or even impossible. From the point of view of calculations it is advantageous that the problem is reformulated in such a way that the Stefan condition is implicitly bound up in new forms of equations and that the heat equations are applied over the whole fixed domain. With both methods it is possible to take into account the temperature range *dT* in which melting or solidification occurs.

In the paper I and II the material properties of the paraffin are assumed to be constant in the solid and liquid phase. Thus, the Eq.(3) gets a form

$$\rho_l c_{pl}\left(\frac{\partial T_l}{\partial t}+\vec{v}\bullet\nabla T_l\right)=k_l\nabla^2 T_l \tag{7}$$

The velocity of the liquid paraffin in the cavity due the buoyancy forces is assumed to be constant. Thus, the natural convection effect in the cavity can be simulated trough a heat transfer coefficient. The term $\left(\rho c_p \vec{v}\bullet\nabla T_l\right)$ is replaced with the term $\left(h\nabla T_l\right)$ in Eq.(7), and the Eqs. (1) and (2) are ignored. Thus, the enthalpy form for energy equation (Eq.(7)) with initial and boundary conditions in melting process is

$$\frac{\partial H}{\partial t}=\frac{k}{\rho}\nabla^2 T+\frac{h}{\rho}\nabla T \tag{8}$$

$$T(x,y,0)=T_i \tag{9}$$

$$T(0,y,t)=T(l,,y,t)=T_w(t) \tag{10}$$

$$\frac{\partial T(x,0,t)}{\partial y}=\frac{T(x,D,t)}{\partial y}=0 \tag{11}$$

where H is the enthalpy, h the convection heat transfer efficient in liquid PCM, l is the length of the storage, and D the height of the storage. The subscript i denotes initial and w the wall. When PCM is in solid state, the last term in Eq.(8) can be ignored.

Marshall (1978, 1979) had experimentally investigated the influence of natural convection on the interface of PCM in a rectangular storage containing paraffin during the melting process. Marshall's results for different paraffins and different boundary conditions was defined as

$$Nu = 0{,}072 Ra^{1/3} \tag{12}$$

where Nu is Nusselt's number $Nu=hS/k_l$. The convection heat transfer coefficient from the fin to the PCM was calculated in Paper III and it took the form:

$$h = 0{,}072 \left[\frac{\left[g\left(\frac{T_w - T_m}{2} \right) \rho_l^2 c_{pl} k_l^2 \beta \right]}{\mu} \right]^{1/3} \tag{13}$$

where β is the expansion coefficient and μ the dynamic viscosity of the PCM. g denotes the acceleration of gravity, and T_m the melting temperature of the PCM.

In the effective heat capacity method the effective heat capacity of the material (c_{eff}) is directly proportional to the energy stored and released during the phase change but inversely proportional to the width of the melting or solidification temperature range. During the phase change the heat capacity of the PCM is

$$c_{eff} = \frac{L}{(T_2 - T_1)} + c_p \tag{14}$$

where T_1 is the temperature at which melting or solidification begins and T_2 the temperature at which the material is totally melted or solidified (temperature range $dT=T_2-T_1$). The heat equation (Eq.(7)) with initial and boundary conditions in the effective heat capacity method takes the form

$$c_p \frac{\partial T}{\partial t} = \frac{k}{\rho} \nabla^2 T + \frac{h}{\rho} \nabla T \tag{15}$$

$$T(x,y,0) = T_i \tag{16}$$

$$T(0,y,t) = T(l,y,t) = T_w(t) \tag{17}$$

$$\frac{\partial T(x,0,t)}{\partial y} = \frac{T(x,D,t)}{\partial y} = 0 \tag{18}$$

where

$$c_p = \begin{cases} c_{ps}, & T < T_1 \\ \dfrac{L}{(T_2 - T_1)} + c_p \ , & T_1 \le T \le T_2 \\ c_{pl}, & T > T_2 \end{cases} \tag{19}$$

In the calculations the temperature ranges in the effective heat capacity method were

- narrow temperature range, melting $dT=T_2-T_1$=27-25°C, solidification $dT=T_2-T_1$=24-26°C and
- wide temperature range, melting $dT=T_2-T_1$=28-21°C, solidification $dT=T_2-T_1$=20-25°C.

The numerical calculation is performed with FEMLAB, which is designed to simulate systems of coupled non-linear and time-dependent partial differential equations (PDEs) in one, two, or three dimensions. The program can be used in the simulation of any system of coupled PDEs in the areas of heat transfer, electromagnetism, structural mechanics, and fluid dynamics. The FEMLAB software operates in the MatLab environment. The program is described in more detail in Paper (I).

In the numerical calculations several of assumptions are made. The assumptions are the following:

- the heat conductivity and density of the phase change material and the enclosure are constant. The values for PCM are chosen to be average values of solid and liquid material properties, (k_p=0.185 W/mK and ρ_p=770 kg/m³);
- the problem is handled two-dimensionally. The heat transfer in the z-direction is assumed to be negligible, and
- the convection heat transfer coefficient in liquid PCM during the solidification process is negligible.

The numerical calculations were performed for the same melting and solidification cycles as in the experiments, and the temperature of the end walls and the boundary conditions, Eqs. (10) and (17), are defined according to experiments.

In the enthalpy method the enthalpy term gets a form $\dfrac{\partial H}{\partial t} = c_p(T)\dfrac{\partial T}{\partial t}$ where the specific heat of the paraffin is continuous and determined according to DSC measurements (see Fig. (2)). The enthalpy method is normally used when accurate specific heat of the PCM in the function of the temperature is not known. The material manufacturers tell normally only material properties in solid and liquid phases, melting and solidification temperatures and latent heat of fusion during the phase change. In that case the effective heat capacity method is more suitable to use when calculating phase change processes.

Table 2 presents the specific heat capacities and the convective heat transfer coefficients for the paraffin used in the numerical calculations in the temperature range of 10-40°C in both the melting and freezing processes.

Table 2. The specific heat and convective heat transfer coefficient of the paraffin in numerical calculations.

Paraffin $c_p(T)$	Melting	Solidification
Enthalpy method	$c_P(T) = \begin{cases} 24T^2 - 515T + 3606, & 10°C \le T < 20°C \\ 145T^3 - 9123T^2 + 191658T - 1344600, & 20°C \le T \le 27°C \\ 11285T^2 - 652160T + 9424300, & 27°C < T \le 29°C \\ 2400, & T > 29°C \end{cases}$ $h=75\ W/m^2K$ when $T>20°C$	$c_p(T) = \begin{cases} 32T^2 - 671T + 4548, & 10°C \le T < 19°C \\ 3206T^2 - 124276T + 1207500, & 19°C \le T \le 23°C \\ -11543T^2 + 536878T - 6197600, & 23°C < T \le 25°C \\ -7374T + 194125, & 25°C < T \le 26°C \\ 2400, & T > 26°C \end{cases}$ $h=0\ W/m^2K$
Effective heat capacity method	$c_p(T) = \begin{cases} 1800, & T \le 21 \\ 21478, & 21 < T \le 28 \\ 2400, & T > 28 \end{cases}$ $h=75\ W/m^2K$ when $T>21°C$ $c_p(T) = \begin{cases} 1800, & T \le 25 \\ 59633, & 25 < T \le 27 \\ 2400, & T > 27 \end{cases}$ $h=69\ W/m^2K$ when $T>25°C$	$c_p(T) = \begin{cases} 1800, & T \le 20 \\ 27220, & 20 < T \le 25 \\ 2400, & T > 25 \end{cases}$ $c_p(T) = \begin{cases} 1800, & T \le 24 \\ 65648, & 24 < T \le 26 \\ 2400, & T > 26 \end{cases}$ $h=0\ W/m^2K$

The specific heat of the paraffin used in different calculation methods and DSC measurements are shown in Fig.5.

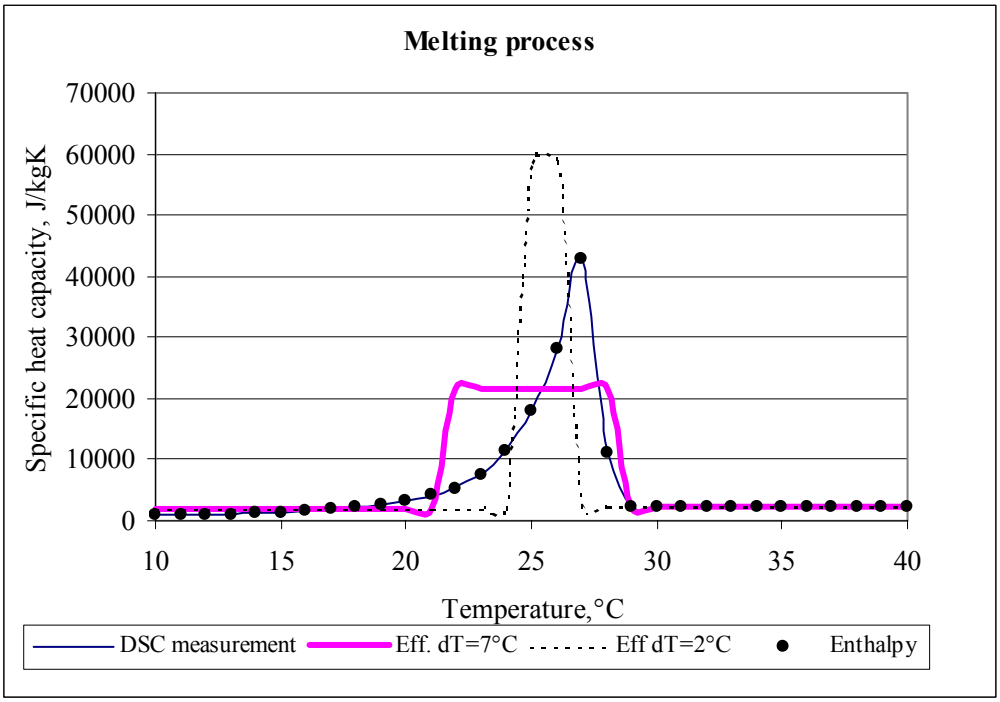

Figure 5. The specific heat of the paraffin in different calculation methods and DSC measurements in melting process.

2.3 Results and discussion

The temperature of the PCM was calculated numerically at eight measurement points in Storage 1. The numerical and experimental results of the temperature of the PCM at Point 4 are presented in Fig. 6. *Exp* denotes experimental results, *Ent* the numerical results calculated with the enthalpy method, *Eff_2* the numerical results calculated with the effective method with a narrow temperature range (dT=2°C), and *Eff_7* the numerical results calculated with the effective method with a wide temperature range (dT=7°C).

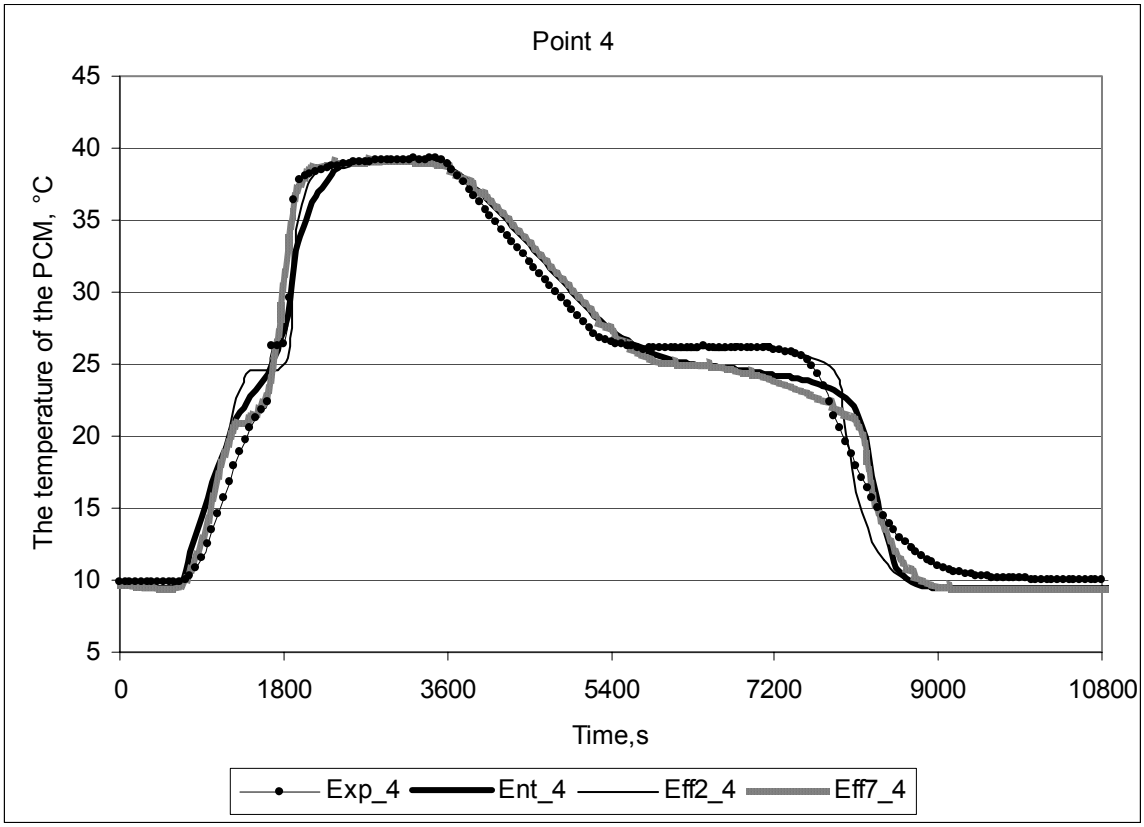

Figure 6. The temperature of the PCM at Measurement Point 4 in PCM Storage 1, without fins.

It can be seen from the Fig.6 that during the melting process all the numerical methods give nearly uniform results for the temperature of the PCM when the PCM is in a solid state. The PCM starts to melt first when the effective heat capacity method with a wide temperature range (*Eff_7*) is used in the calculations. The melting starts approximately at 20°C. However, quite soon the effect of natural convection renders uniform the temperature development of the PCM in all the numerical methods. The effect of natural convection in the liquid PCM seems to be modelled well in the numerical methods.

During the solidification process all the numerical methods give uniform results for the temperature of the PCM in a liquid state. When solidification begins the effective heat capacity method with a wide temperature range gives nearly uniform results with the enthalpy method but differs from the results achieved with the effective heat capacity with a narrow phase change range. However, the effective heat capacity method with a narrow temperature range follows the experimental results most closely when phase change occurs. After solidification the solid PCM freezes a little too fast compared to experimental results.

Fig. 7 shows the temperature of the PCM at Point 10 in PCM Storage 2, with fins.

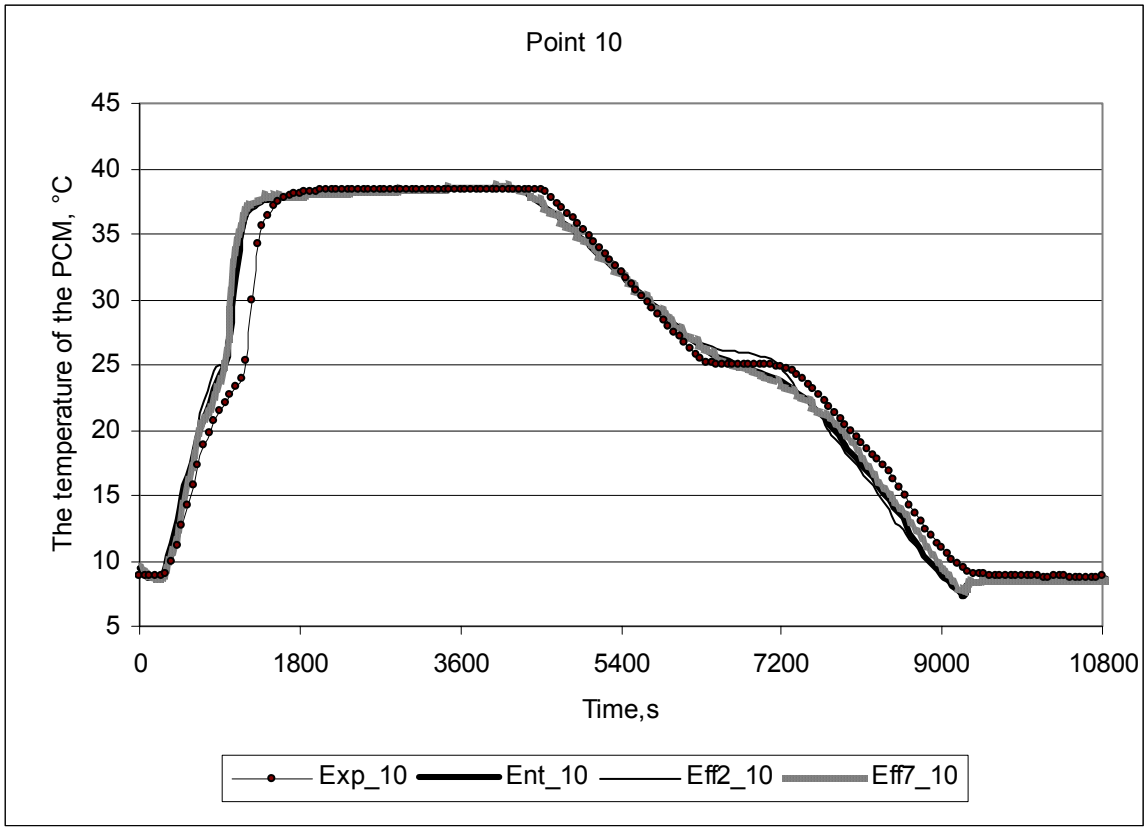

Figure 7. The temperature of the PCM at Measurement point 10 in the PCM storage with fins.

The same phenomena which were observed in the storage without fins can also be seen in the results (Fig.7) obtained for the storage with fins. The PCM heats up and cools down too fast in the solid state when the numerical results are compared to the experimental results.

In the solidification process the numerical results for the temperature of the PCM follow well the experimental results when the PCM is in a liquid state. The conclusion is that the effective heat capacity method with a narrow temperature range gives the most precise result for the temperature of the PCM compared to numerical results.

The numerical and experimental results differ a little from each other. It seems that the biggest error is made when the material is solid. The most evident reason for the difference may be in the thermal contact resistance between the coldplate and the PCM container. Thermal contact resistance was not taken into account in the simulations. The material properties of the PCM are also assumed to be constant in the calculations. If the temperature dependent material properties are known, the numerical methods will give more precise results for the temperature of the PCM. The volume change during phase change was not taken into account in the numerical calculations. The volume of the material increases upon melting and shrinks upon freezing process. This may cause the differences between numerical and experimental results. Another reason for the differences may be in the placement of the thermocouple. The storage is filled with

liquid PCM. The placement of the thermocouple may have been slightly changed. After the storage is filled up it is impossible to check the placement of the thermocouple.

However, the error when the numerical and experimental results were compared to each other is relatively small. The most precise numerical method for the technical grade paraffin used in these experiments seems to be the effective heat capacity method with a narrow temperature range (dT=2°C).

It seems that natural convection is well modelled in the numerical models (Eq.(8) and (15)). The natural convection in the liquid PCM is quite often assumed to be negligible in numerical calculations. Fig. 8 shows the experimental and numerical results of the temperature of the PCM at point 4 in the storage without the fins. The numerical results are calculated using the effective heat capacity method with a narrow phase change temperature range both with the natural convection effect and without the natural convection effect.

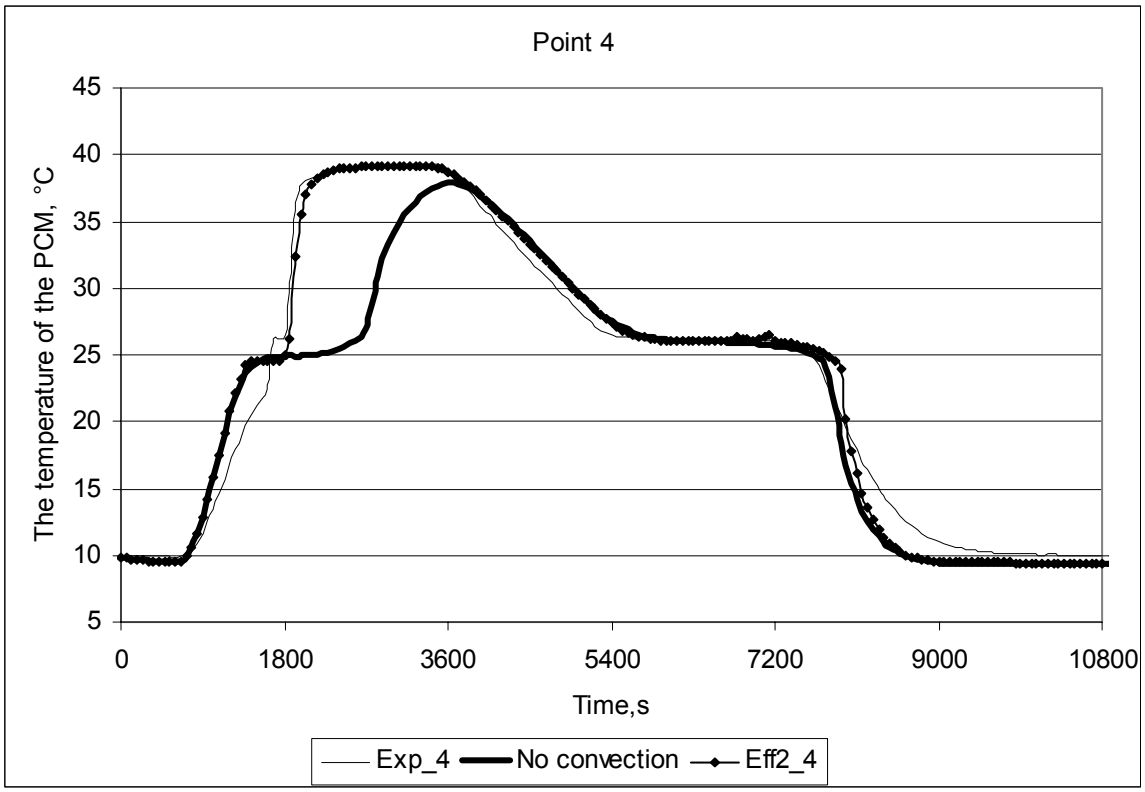

Figure 8. The numerical results both with natural convection and without natural convection and the experimental results for the temperature of the PCM.

From the results in Fig. 8 it is possible to see that the assumption used for the natural convection coefficient (Eqs.(8) and (15)) gives a fairly good estimation for the behavior of the PCM during the melting process. When the effect of natural convection is neglected in the calculation, the PCM heats up to the maximum coldplate temperature twice as slowly as it actually takes in reality. The error made is considerable and the numerical model is not performing well if natural convection is not occurring in the liquid PCM during the melting process.

FEMLAB seems to be very suitable for solving different kinds of phase change problems. The program saves time and effort. It makes it possible to change the geometry of the storage easily and, for example, different kinds of heat transfer enhancement structures, such as fins and honeycombs, can be modelled and the effect of the structure can be seen quickly and easily.

During the measurements the thermal images of the PCM surface were recorded at one minute intervals. Fig. 9 depicts the experimental deviation between the thermocouple and IR measurements at Point 12 in Storage 2.

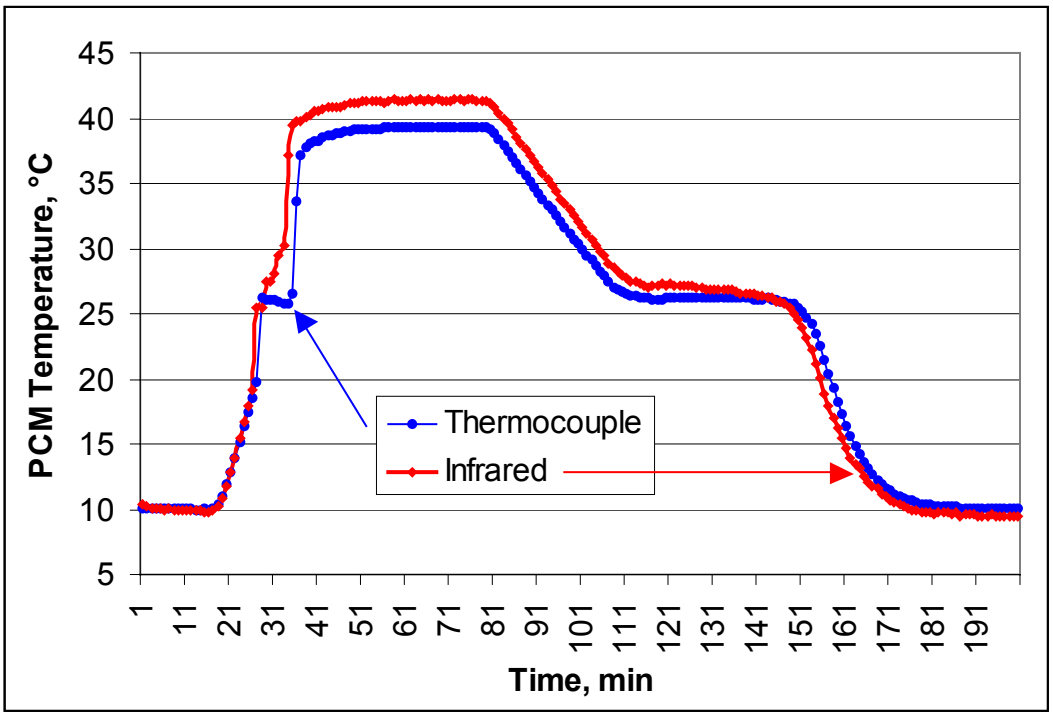

Figure 9. 2-D temperature distribution in PCM Storage 2 at Point 12.

The IR image was asymmetrical due to the camera being tilted so as to avoid reflections from the ZnSe window surface. The temperature difference between the results of the IR camera and the thermocouple was approximately one degree, due to an internal calibration error in the camera, which was experimentally verified. Although in this study the thermocouples provided more reliable results than the IR camera, the feasibility of infrared thermography and its capability for quantitative visualisation using infrared windows was however confirmed.

3 ANALYTICAL MODEL FOR MELTING IN A SEMI-INFINITE PCM STORAGE WITH AN INTERNAL FIN

The objective of Paper III was to examine the melting process in a semi-infinite PCM storage with a fin. A simplified analytical model based on a linear, transient, thin-fin equation was presented which predicted the solid-liquid interface location and temperature distribution of the fin. The two-dimensional problem was simplified into a one-dimensional problem and the equations were solved numerically by means of the finite element method. The analytical results were compared to the numerical results calculated with FEMLAB.

3.1 Mathematical formulation

The construction of a semi-infinite PCM storage with an internal fin is presented in Fig. 10. The storage is divided into two regions. In Region 1, the heat is transferred mainly in the x-direction and in Region 2 in the y-direction. In Region 1, the only heat source is the constant-temperature end wall. Here the fin does not influence the melting process. In Region 2, both the wall and the fin transfer heat from the wall to the phase change material.

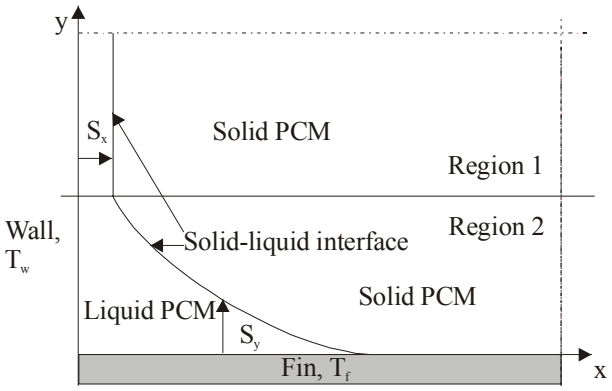

Figure 10. Semi-infinite phase change material storage with a fin.

The end wall is suddenly exposed to a temperature which is higher than the melting temperature of the PCM. Heat is transferred from the wall and through the fin to the PCM. There exist three stages in the melting process near the fin: first, pure conduction from the end wall and the fin, then conduction from the fin with some natural convection from the end wall, and finally, only natural convection from the fin. The natural convection begins to dominate the heat transfer mode from the horizontal fin to the solid-liquid interface when Rayleigh number is $Ra \geq 1708$. However, the fin tends to

decrease natural convection from the end wall due to the decreasing temperature gradient in the liquid.

Several assumptions are made in order to simplify the non-linear heat transfer problem. The assumptions are the following:

1. the solid PCM and the fin are initially at the melting temperature of the phase change material $T_m=T_s=T_f$. Therefore, heat conduction in solid PCM is considered to be negligible;
2. the end wall temperature T_w is kept constant and it is higher than the melting temperature of the phase change material T_m;
3. the temperature distribution of the thin fin is considered to be one-dimensional in the x-direction;
4. the sensible heat of liquid PCM is assumed to be negligible. The latent heat of fusion is assumed to be the principal mode of energy storage;
5. in Region 1 the heat is transferred from the wall to the solid-liquid interface one-dimensionally in the x-direction. The main heat transfer mode is assumed to be conduction in liquid PCM;
6. in Region 2 heat transfer is assumed to be one-dimensional from the fin to the solid-liquid interface in the y-direction because the fin plays the most important role in melting PCM in Region 2. The main heat transfer mode is assumed to be natural convection in liquid PCM. Conduction is assumed to be negligible, and
7. the physical properties for the phase change material and for the fin are assumed to be constant.

In Region 1 the heat is transferred mainly in the x-direction. Therefore, the melting or solidification is handled as a one-dimensional one-phase Stefan problem. The heat equation (Eq. (3)) for the liquid PCM and the heat balance for the solid-liquid interface (Eq. (5)) can be rewritten as (Alexiades et al. 1993):

$$\frac{\partial^2 T_l}{\partial x^2} = \frac{1}{\alpha_l}\frac{\partial T_l}{\partial t} \qquad ,t>0 \qquad (20)$$

$$T_l(x,0)=T_m \qquad (21)$$

$$T_l(0,t)=T_w \qquad (22)$$

$$(\rho L)_l \frac{\partial S_x(t)}{\partial t} = -k_l \frac{\partial T_l(S_x,t)}{\partial x} \qquad ,t>0 \qquad (23)$$

$$S_x(0)=0 \qquad (24)$$

$$T_l(S_x,t)=T_m \qquad (25)$$

where $S_x(t)$ is the location of the solid-liquid interface in the x-direction as a function of time.

In Region 2 the heat is transferred mainly in the y-direction. The temperature distribution of the fin with initial and boundary conditions is defined as

$$\left(\rho c_p\right)_f D\frac{\partial T_f}{\partial t} = k_f D\frac{\partial^2 T_f}{\partial x^2} - h(T_f - T_m) \qquad ,t>0 \qquad (26)$$

$$T_f(x,0)=T_m \qquad (27)$$

$$T_f(0,t)=T_w \qquad (28)$$

$$T_f(\infty,t)=T_m \qquad (29)$$

where T_f is the temperature of the fin, h the heat transfer coefficient from the fin to the solid-liquid interface, and D is the half-thickness of the fin.

The heat balance for the solid-liquid interface is written with an initial condition as

$$\left(\rho L\right)_l \frac{\partial S_y}{\partial t} = \frac{k_l}{x}(T_w - T_m)\frac{\partial S_y}{\partial x} + h(T_f - T_m) \qquad ,t>0 \qquad (30)$$

$$S_y(0)=0 \qquad (31)$$

where S_y is the distance from the fin to the solid-liquid interface in the y-direction.

The convective heat transfer coefficient gained the following form in Paper III:

$$Nu = 0{,}072 Ra^{1/3} \qquad (32)$$

where Nu is Nusselt's number $Nu=hS/k_l$. The convection heat transfer in liquid PCM is assumed to be following:

$$h = 0{,}072\left[\frac{\left[g\left(\frac{T_w - T_m}{2}\right)\rho_l^2 c_{pl} k_l^2 \beta\right]}{\mu}\right]^{1/3} \qquad (33)$$

3.2 Solution

In Region 1 the Stefan problem (Eqs. (20)-(25)) has a well-known analytical solution provided by Neumann (Alexiades et al. 1993). The location of the solid-liquid interface can be solved from Eq. (34):

$$S_x(t) = 2\lambda\sqrt{\alpha_l t} \tag{34}$$

where λ is a root of the transcendental equation.

$$\lambda e^{\lambda^2} erf(\lambda) = \frac{St_l}{\sqrt{\pi}} = \frac{c_{pl}(T_w - T_m)}{L\sqrt{\pi}}. \tag{35}$$

where *St* is the Stefan number.

In Region 2, the equations (Eqs. (26)-(31)) for the temperature distribution of the fin are solved explicitly. The problem is a parabolic partial differential initial boundary value problem and it is possible to find an exact solution for the equations. The solution for the temperature distribution of the fin is

$$T_f(x,t) = \frac{(T_w - T_m)\left\{e^{Bt-\sqrt{\frac{Bx^2}{A}}} - \frac{1}{2}e^{Bt-\sqrt{\frac{Bx^2}{A}}}\left(1 - e^{2\sqrt{\frac{Bx^2}{A}}} + erf\left[\frac{x}{2\sqrt{At}} - \frac{\sqrt{Bx^2 t}}{x}\right] + e^{2\sqrt{\frac{Bx^2}{A}}} erf\left(\frac{x}{2\sqrt{At}} + \frac{\sqrt{Bx^2 t}}{x}\right)\right)\right\}}{e^{Bt}} + T_m \tag{36}$$

where $A = \frac{k_f}{(\rho c_p)_f}$ and $B = \frac{h}{(\rho c_p)_f D}$. (37)

The energy balance for the PCM interface location in the y-direction (Eq.(30)) is a first-order partial differential equation. It can be solved with the method of characteristics for quasilinear equations (Guenther et al. 1988). The solution for the fin temperature distribution Eq. (36) is placed into Eq. (30), which gives, for the interface location S_y in the y-direction,

$$S_y(x,t) = h(T_f - T_m)x\left(\frac{-bx + \sqrt{(bx)^2 + 2abt}}{ab}\right). \tag{38}$$

where $a = k_l(T_w - T_m)$ and $b = \rho_l L$ (39)

The method of characteristics for quasilinear equations has some limitations when solving partial differential equations and in this case the solution is not valid when x approaches zero. However, in this model, when x approaches zero the Neumann solution S_x for interface location (Eqs. (34) and (35)) is valid instead of Eq. (38).

3.3 Results and discussion

The derived analytical solution (Eqs. (36) and (37)) for the temperature distribution of the fin was compared to the numerical solution in order to verify the accuracy of the analytical solution. The equations of the fin temperature distribution with initial and boundary conditions (Eqs. (26)-(29)) were solved numerically with FEMLAB.

A test case was chosen. In the test case the physical properties of laboratory-grade pure n-octadecane paraffin were used as initial values, because of its relatively narrow melting region at T_m=28°C. The fin was assumed to be aluminium. The initial temperature of the PCM and the fin was assumed to be 28°C and the end wall temperature T_w=48°C. The half-thickness of the fin was assumed to be D=1 mm. The heat transfer coefficient got a value h=70.03 W/m^{2}K (Eq.(33)) in the calculations.

The derived analytical and numerical results for the temperature distribution of the fin are shown in Fig. 11 at time step t=3600 s.

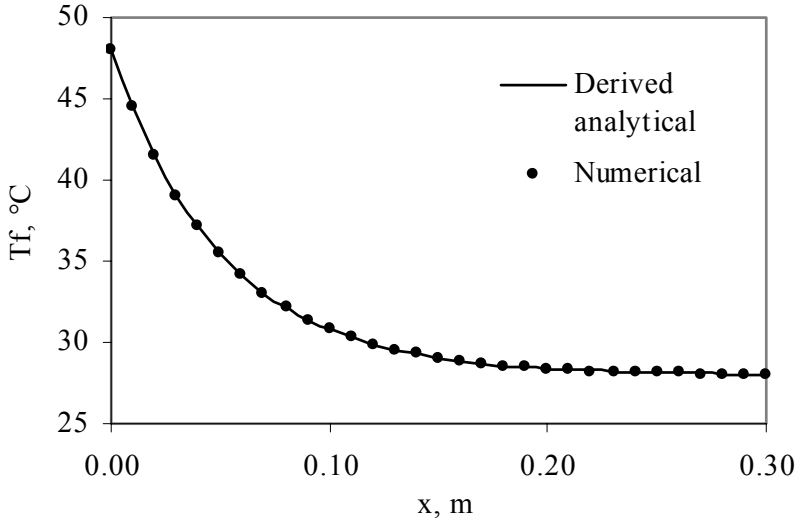

Figure 11. The analytical and numerical results for the temperature of the fin T_f at t=3600 s.

The difference between the analytical and numerical solutions is extremely small, because the analytical solution for the problem is an exact solution. An analytical solution is more precise than the numerical solution achieved with FEMLAB. However, the derived analytical solution for the temperature distribution of the fin gives

satisfactory results. The heat transfer coefficient from the fin to the solid-liquid interface is assumed to be constant in the model. In reality it is a function of the temperature difference T_f-T_m. At small x values the value of the heat transfer coefficient is too low and at large x values it is too high. Thus, the solid-liquid interface location is also underestimated at small x values and overestimated at large x values. However, the error made is small.

The Neumann solution for the solid-liquid interface location is known to be an exact solution (Eqs. (34) and (35)) in Region 1. However, it is known that the Neumann solution underestimates the speed of the solid-liquid interface S_x because the natural convection in the melted PCM is ignored in the model. Natural convection assists in the melting of the PCM and the solid-liquid interface is ahead of the interface achieved with the Neumann solution.

In Region 2 the derived analytical solution for the interface location (Eqs. (38) and (39)) should be validated by comparing the derived analytical results to the numerical results calculated with FEMLAB at t=3600 s. The results are shown in Fig. 12.

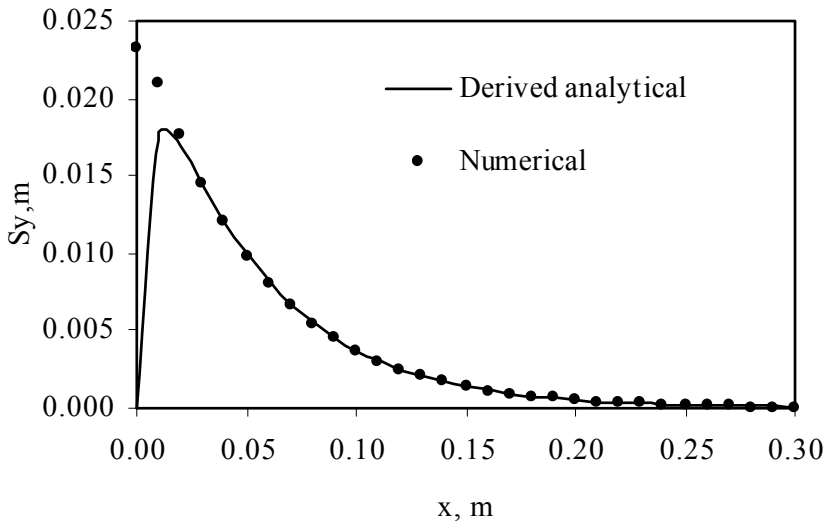

Figure 12. Analytical and numerical results for the solid-liquid interface location S_y at t=3600 s in region 2.

The numerical solution for the problem gives the same result as the derived analytical solution, except near the wall (x approaches zero). However, near the wall in Region 1 the location of the solid-liquid interface is solved with the Neumann solution.

The effect of the assumption that heat is transferred only by natural convection between the fin and PCM in Region 2 was studied by comparing the analytical results to the following numerical results:

- Case 1. Heat transfers first by conduction (Ra≤1708) and later by natural convection (Ra>1708) from the fin;

- Case 2. Heat transfers by conduction from the fin to the solid-liquid interface, and
- Case 3. The phase change phenomenon is ignored in the calculations.

The cases are described in more detail with mathematical formulations in Paper III. The analytical and numerical results in different cases at t=3600 s are shown in Fig. 13.

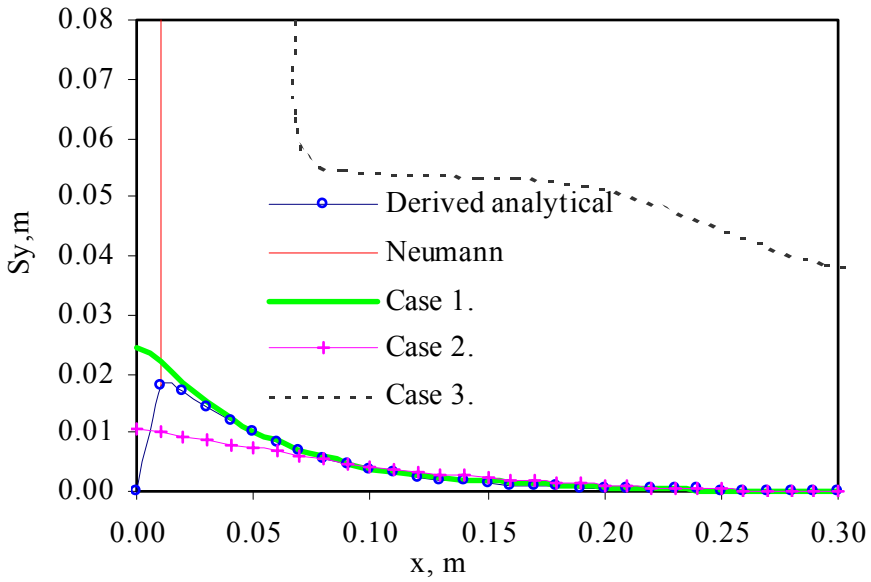

Figure 13. The analytical and numerical results in Test Cases 1-3 at t=3600 s.

In Case 1, the solid-liquid interface S_y is slightly ahead of the interface of the analytical solution. In Case 2, the interface location S_y is a long way behind the derived analytical solution. Natural convection enhances heat transfer and accelerates melting. Therefore, it should be taken into consideration. Otherwise the model considerably underestimates the solid-liquid interface location. In Case 3, it is obvious that the interface in which the material's temperature differs from its initial temperature is situated substantially ahead of the solid-liquid interface achieved with an analytical solution because there is no effect resulting from the latent heat of fusion.

All in all, the assumption that the prime heat transfer mode is natural convection is justified. The error made is small when the conduction that exists in the early stages is ignored in the model. Conduction at the beginning of the process has a very small effect on the liquid-solid interface location.

4 APPROXIMATE ANALYTICAL MODEL FOR SOLIDIFICATION IN A FINITE PCM STORAGE WITH INTERNAL FINS

The work done in Paper III was extended in Paper IV in order to deal with the solidification process. The aim of this paper was to present a simplified analytical model which predicted the solid-liquid interface location and temperature distribution of the fin in the solidification process with a constant end-wall temperature in a finned two-dimensional PCM storage. In addition to the one-dimensional analytical model, the heat transfer in the PCM storage was calculated with a simplified one-dimensional numerical model and a two-dimensional numerical model. The one-dimensional numerical calculation was carried out with FEMLAB and the two-dimensional numerical calculation, based on the enthalpy method, was implemented in the Digital Fortran 5.0 environment. By comparing the results of different methods it was possible to draw conclusions regarding the accuracy of the one-dimensional analytical model. A factor, called the fraction of solidified PCM, was also introduced in the paper.

4.1 Mathematical formulation

Consider Fig. 1. The storage is initially at the solidification temperature of the PCM. The side walls are suddenly subjected to a lower temperature than its solidification temperature. The PCM starts to solidify and the heat released during phase change is transferred through the fin and PCM from the solid-liquid interface to the environment.

Due to the non-linear, unsteady nature of the problem several assumptions have been made in order to simplify the two-dimensional heat transfer problem, as in Paper III. The assumptions were the following:

1. initially, the liquid PCM and the fin are at the solidification temperature of the phase change material $T_m=T_l=T_f$. Therefore, the heat conduction and natural convection in the liquid PCM are considered to be negligible. The sole means of heat transfer is by conduction in the solid PCM;
2. the solidification temperature (T_m) is assumed to be constant. In reality, a phase change material has a solidification range (ΔT_m);
3. the temperature distribution of the fin is considered to be one-dimensional in the x-direction because the fin is thin and the conductivity of the fin material is high;
4. in Region 1, heat transfer is one-dimensional and takes place only in the x-direction. The fin does not affect heat transfer in this region;
5. in Region 2, the solid-liquid interface moves only one-dimensionally in the y-direction because the heat is mainly transferred through the fin to the environment;

6. in Region 2, the sensible heat of solid PCM is assumed to be negligible. The latent heat of fusion is assumed to be the principal mode of energy storage. In Region 1, the sensible heat is taken into account, and
7. the physical properties of the phase change material and the fin, such as heat conductivity, heat capacity, and density, are assumed to be constant.

In Region 1 the solidification was handled as a one-dimensional one-phase Stefan problem. In a one-phase Stefan problem the heat equation for a solid phase change material and for a solid-liquid interface with an initial and boundary conditions is (Alexiades et al. 1993):

$$\frac{\partial^2 T_s}{\partial x^2} = \frac{1}{\alpha_s}\frac{\partial T_s}{\partial t} \qquad ,t>0,\ \ 0 \le x \le l_f \qquad (40)$$

$$-(\rho L)_s \frac{\partial S_x(t)}{\partial t} = -k_s \frac{\partial T_s(S_x,t)}{\partial x} \qquad ,t>0 \qquad (41)$$

$$S_x(0)=0 \qquad (42)$$

$$T_s(S_x,t)=T_m \qquad (43)$$

$$T_s(0,t)= T_s(l_f,t)= T_w \qquad (44)$$

where l_f is the length of the fin and s denotes solid.

In Region 2 the heat equation for the temperature of the fin was written with initial and boundary conditions as

$$(\rho c_p)_f D\frac{\partial T_f}{\partial t} = k_f D\frac{\partial^2 T_f}{\partial x^2} - \frac{k_s}{S_y}(T_f - T_m) \qquad ,t>0 \qquad (45)$$

$$T_f(x,0)=T_m \qquad (46)$$

$$T_f(0,t)= T_f(l_f,t)=T_w \qquad (47)$$

The energy balance for the solid-liquid interface recession in the y-direction is

$$-(\rho L)_s \frac{\partial S_y}{\partial t} = \frac{k_s}{x}(T_w - T_m)\frac{\partial S_y}{\partial x} + \frac{k_s}{S_y}(T_f - T_m) \qquad ,t>0 \qquad (48)$$

$$S_y(x,0)=0. \qquad (49)$$

Eqs. (39)-(43) were converted into a dimensionless form. The following dimensionless variables were introduced:

$\theta = \frac{T - T_m}{T_w - T_m}$, dimensionless temperature distribution

$\tau = \frac{k_f t}{(\rho c_p)_f l_f^2}$, dimensionless time

$\gamma = \frac{S_y}{l_c}$, dimensionless rate of solid-liquid interface recession

$\eta = \frac{x}{l_f}$, dimensionless x-coordinate

$\lambda = \frac{l_f}{l_c}$, cell aspect ratio

$\Psi = \frac{D}{l_c}$, dimensionless half-thickness of the fin

$\kappa = \frac{k_s}{k_f}$, ratio of heat conductivities and

$\xi = \frac{(\rho c_p)_f (T_w - T_m)}{-L\rho_s}$, modified Stefan number (50)

Eqs. (45)-(49), rewritten using the dimensionless variables, took the form:

$$\frac{\partial \theta}{\partial \tau} = \frac{\partial^2 \theta}{\partial \eta^2} - \frac{\lambda^2 \kappa}{\Psi} \frac{\theta}{\gamma} \qquad ,\tau>0 \qquad (51)$$

$$\theta(\eta, 0) = 0 \qquad (52)$$

$$\theta(0, \tau) = \theta(1, \tau) = 1 \qquad (53)$$

$$\frac{\partial \gamma}{\partial \tau} = \frac{\xi \kappa}{\eta} \frac{\partial \gamma}{\partial \eta} + \xi \kappa \lambda^2 \frac{\theta}{\gamma} \qquad ,\tau>0 \qquad (54)$$

$$\gamma(\eta, 0) = 0 \,. \qquad (55)$$

Eqs. (40)-(44) and (51)-(55) form the basis for the simplified one-dimensional model.

4.2 Solution

In Region 1 the distance of the solid-liquid interface from the left end wall can be solved from Eqs. (40)-(44) (Alexiades et al 1993):

$$S_{x=0} = 2\lambda\sqrt{\alpha_s t} \tag{56}$$

where λ is a root of the transcendental equation

$$\lambda e^{\lambda^2} erf(\lambda) = \frac{St_l}{\sqrt{\pi}} = \frac{c_p(T_w - T_m)}{-L\sqrt{\pi}}\,. \tag{57}$$

Due to the symmetry, the distance of the solid-liquid interface from the right end wall is

$$S_{x=Lf} = l_f - S_{x=0}\,. \tag{58}$$

In Region 2, for the dimensionless equations (51)-(55) no mathematically exact solution exists. Eq. (51) is a parabolic partial differential equation and it was impossible to solve it with known methods because the dimensionless rate of the solid-liquid interface recession γ is a variable in the equation. Eq. (51) shows that γ is a function of the dimensionless place η and time τ. The following assumptions are made in order to make the dimensionless equations solvable:

1. the dimensionless rate of the solid-liquid interface recession γ is assumed to be constant in Eq. (51) and at the same time the dimensionless temperature distribution θ is a function of the dimensionless time. By introducing a new parameter $\nu = \frac{\lambda^2\kappa}{\Psi\gamma}$, Eq. (51) is rewritten in solvable form

$$\frac{\partial\theta}{\partial\tau} = \frac{\partial^2\theta}{\partial\eta^2} - \nu\theta \qquad ,\tau>0; \tag{59}$$

2. at the same time the dimensionless temperature distribution θ is assumed to be constant in Eq. (54) and the dimensionless rate of the solid-liquid interface recession γ is assumed to be only the function of dimensionless time. Hence, Eq. (54) can be rewritten as

$$\frac{\partial\gamma}{\partial\tau} = \xi\kappa\lambda^2\frac{\theta}{\gamma} \qquad ,\tau>0. \tag{60}$$

Eq. (59) is a parabolic partial differential equation and its solution with given initial and boundary conditions is well-known (Carslaw et al. 1959):

$$\theta = \frac{\cosh((\eta - 0.5)\sqrt{v})}{\cosh(0.5\sqrt{v})} - \frac{4}{\pi e^{v\tau}} \sum_{n=0}^{\infty} \frac{(-1)^n e^{-(2n+1)^2 \pi^2 \tau}}{(2n+1)\left[1 + \left\{v/((2n+1)^2 \pi^2)\right\}\right]} \cos((2n+1)\pi(\eta - 0.5)) \tag{61}$$

The dimensionless rate of the solid-liquid interface recession γ is solved from Eqs. (60) and (55) to give

$$\gamma = \sqrt{2\xi\kappa\lambda^2\theta\tau}\,. \tag{62}$$

Eqs. (61) and (62) were solved and the solution for the dimensionless temperature distribution of the fin and the dimensionless rate of the solid-liquid interface recession was found.

The fraction of solidified PCM was presented in Paper IV. It describes how much of the storage is solidified after a certain time. The factor takes values between 0 (the storage is totally liquid) and 1 (the storage is totally solid).

The factor is defined as the volume of the solidified PCM related to the total volume of PCM in the storage:

$$\varepsilon = \frac{2S_x\left(l_c - D - S_y\right) + \bar{S}_y\, l_f}{(l_c - D) l_f} \tag{63}$$

where $\bar{S}_y$ is the average value of the solid-liquid interface location in the y-direction along the fin length and S_x and $\bar{S}_y$ can be calculated from Eqs. (56)-(58) and Eqs. (61) and (62).

4.3 Results and discussion

To find out the accuracy and performance of the one-dimensional model and the analytical solution, the location of the solid-liquid interface and the temperature of the fin were calculated using three different methods:

1. a simplified one-dimensional analytical model;
2. a simplified one-dimensional numerical model, and
3. a two-dimensional numerical model.

Analytical results were calculated from Eqs. (61) and (62). In Eq. (61) three terms of series was taken into account in calculating analytical results. The one-dimensional numerical results were calculated with FEMLAB using Eqs. (45)-(49). The two-

dimensional numerical calculation was based on the enthalpy method and it was implemented in the Digital Fortran 5.0 environment. The enthalpy method was used in a particular way so that the only unknown variable was the temperature of the phase change material and the solidification occurred at a uniform temperature (Zivkivic et al. 2001). The enthalpy method is presented in more detail in Paper IV.

The procedure used to check the accuracy is presented in Fig. 14.

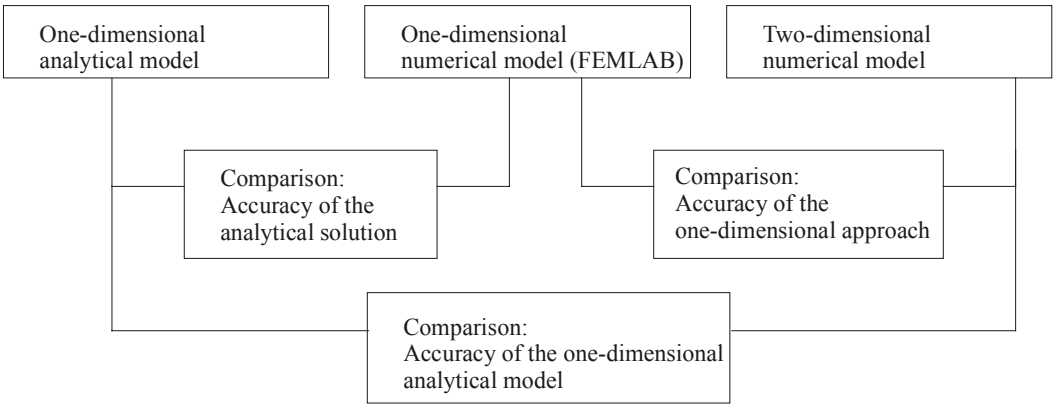

Figure 14. Methodology to find out the effect of different simplifications.

Six different test cases were chosen. In the test cases laboratory-grade pure n-octadecane paraffin with an aluminium fin (3 cases) and a commercial-grade salt hydrate (Climsel 23) with a steel fin (3 cases) were chosen. The solidification temperature of the N-octadecane paraffin was set at T_m=28°C and that of the salt hydrate at T_m=23°C.

In the test cases the initial temperature of the storage was the solidification temperature of the PCM and the PCM was in a liquid state. The temperature difference between the PCM and the wall (T_m-T_w) was fixed at 15°C in all cases. The half-thickness D of the fin had a constant value of 0.5 mm. Otherwise, three different λ values were used. The calculation time was also varied. The geometry, initial temperatures, materials and calculation times used in different test cases are shown in Table 3.

Table 3. The geometry of the storage, initial temperatures, materials and calculation time used in different test cases.

	Case 1	Case 2	Case 3	Case 4	Case 5	Case 6
PCM	Paraffin	Paraffin	Paraffin	Salt hydrate	Salt hydrate	Salt hydrate
Fin	Aluminium	Aluminium	Aluminium	Steel	Steel	Steel
Tm,°C	28	28	28	23	23	24
Tw,°C	13	13	13	8	8	8
lf,m	0.01	0.05	0.05	0.01	0.05	0.05
lc,m	0.05	0.05	0.01	0.05	0.05	0.01
λ=lf/lc	**0.2**	**1**	**5**	**0.2**	**1**	**5**
D,m	0.0005	0.0005	0.0005	0.0005	0.0005	0.0005
t,s	723	1085	1085	169	4226	1127
τ,–	500	30	30	30	30	6

In Fig. 15a-f the temperature distributions of the fin and in Fig. 16a-f the solid-liquid interface locations in different test cases are shown.

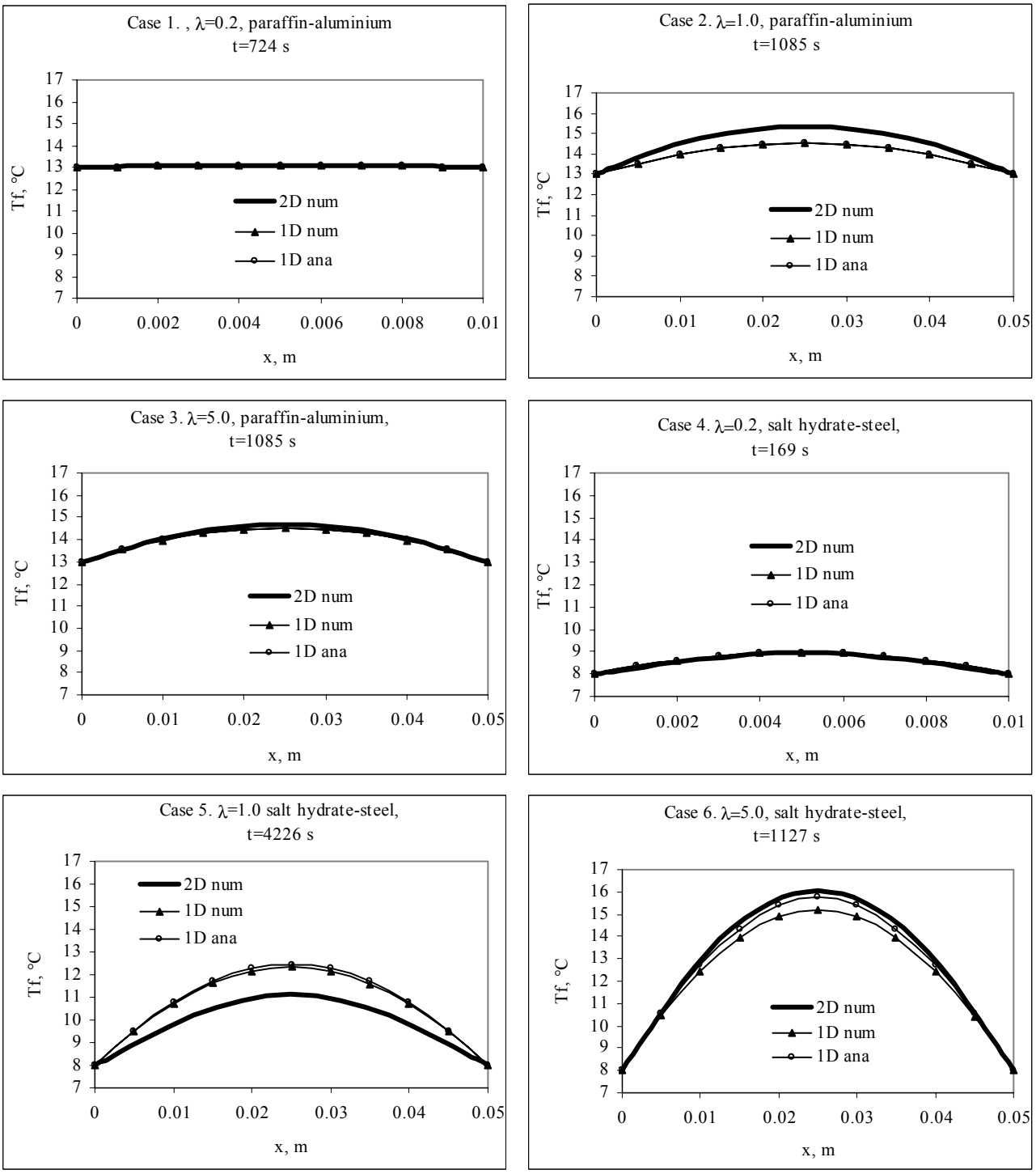

Figure 15a-f. The temperature distribution of the fin calculated with one-dimensional analytical and numerical methods and the two-dimensional numerical method.

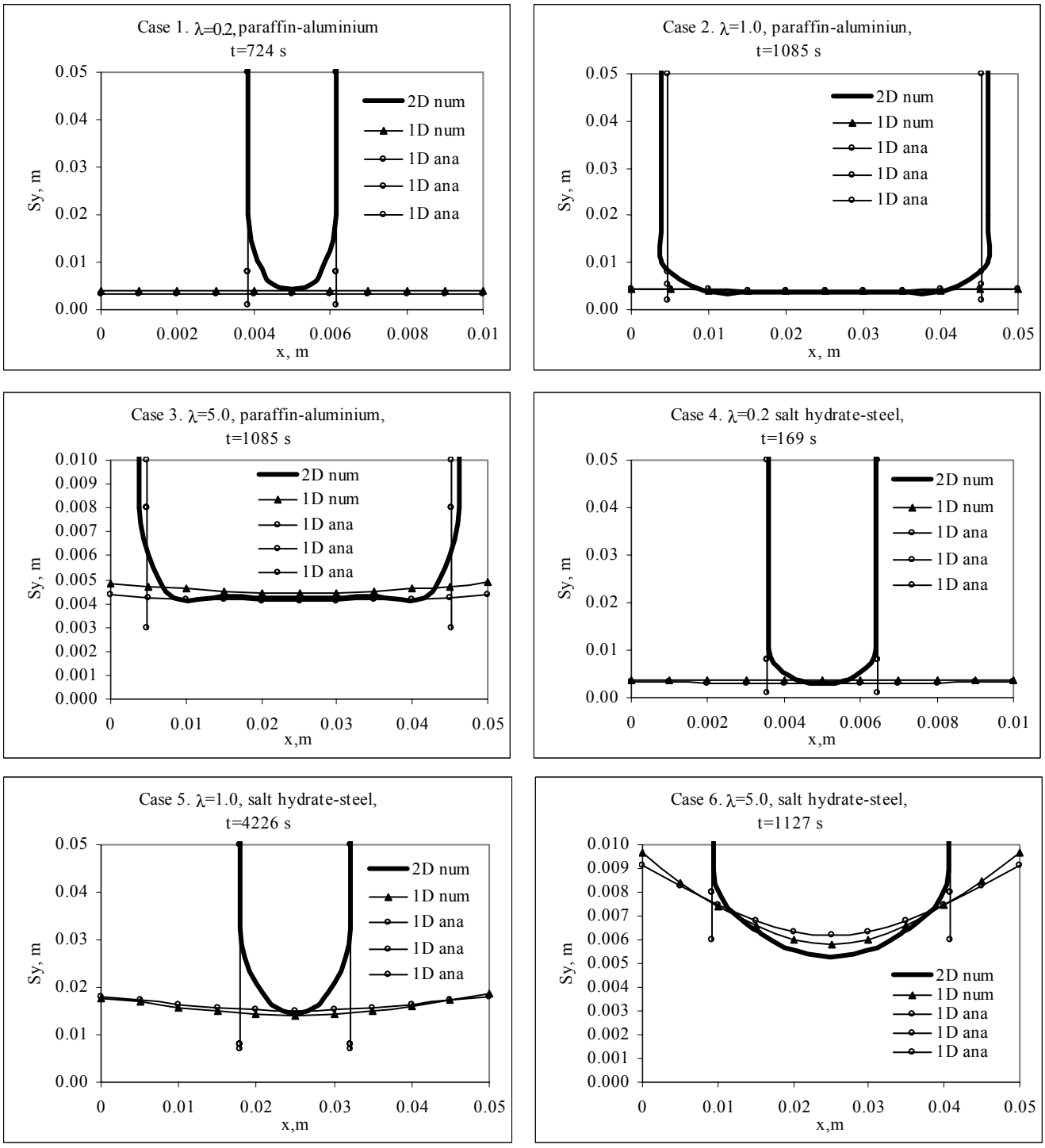

Figure 16a-f. The location of the solid-liquid interface calculated with one-dimensional analytical and numerical methods and the two-dimensional numerical method.

The results show that the geometry of the storage seems to be one of the most important factors in explaining the performance of the developed one-dimensional model. When the width-to-height ratio (λ) is small or large, the accuracy of the one-dimensional approach is relatively good because the heat transfer is near to a one-dimensional model in the x-direction (λ is small) or the y-direction (λ is large). When λ is equal to one, the heat is effectively transferred both in the x- and y-directions. By using a one-dimensional approach instead of a two-dimensional approach, the accuracy is slightly reduced. However, the results are still satisfactory, especially for the solid-liquid interface location.

The assumptions made (Eqs. (59) and (60)) in order to make possible the analytical solution have a minor influence on the results. Thus, the accuracy of the analytical solution is good. The assumptions made in simplifying the two-dimensional heat transfer problem into a one-dimensional form affect the accuracy to a greater extent than the assumptions made when solving the one-dimensional equations analytically.

The fractions of solidified PCM calculated from the one-dimensional analytical (Eq. (63)) and two-dimensional numerical results in different test cases are shown in Table 4.

Table 4. The fractions of solidified PCM calculated with the one-dimensional analytical and two-dimensional numerical models in different test cases.

Case	$\lambda = l_f/l_c$	Time	Tw-Tm	D	Fraction Analytical	Fraction Numerical	Error
	-	s	°C	m	-	-	%
Case 1, para	0.2	724	15	0.0005	0.787	0.799	-1.2
Case 2,para	1	1085	15	0.0005	0.258	0.233	2.4
Case 3,para	5	1085	15	0.0005	0.543	0.539	0.4
Case 4, salt	0.2	169	15	0.0005	0.733	0.749	-1.7
Case 5, salt	1	4226	15	0.0005	0.804	0.826	-2.3
Case 6,salt	5	1127	15	0.0005	0.819	0.791	2.8

The difference between the analytical and numerical fractions of solidified PCM is less than ± 2.8% in all cases. It seems that the factor (Eq. (63)) gives a good picture of how much of the storage is solidified. The factor is useful when dimensioning PCM storages and also when different geometries are compared with each other. However, the fraction of solidified PCM is a bulk measure and it neglects microscopic effects in PCM operation. The factor is a useful tool, together with analytical results that indicate the location of the solid-liquid interface in the pre-design stage of the storage.

5 APPROXIMATE ANALYTICAL MODEL FOR THE TWO-PHASE SOLIDIFICATION PROBLEM IN A FINNED PHASE CHANGE MATERIAL STORAGE

Paper V extended the one-dimensional analytical approach of the two-dimensional heat transfer problem in a finned PCM storage to cases where the storage is initially at a higher temperature than the PCM's solidification temperature. The paper presented a simplified analytical model based on a linear, transient, thin-fin equation which predicted the solid-liquid interface location and temperature distribution of the fin in a solidification process with a constant end wall temperature in a finite PCM storage.

In addition to the one-dimensional analytical approach, the problem was also solved numerically in two dimensions by using the effective heat capacity method. The calculation with the effective heat capacity method was carried out with FEMLAB.

5.1 Mathematical formulation

In Paper V the storage examined had the same structure as the storage in Paper IV. The storage was presented in Fig. 1. In the storage the liquid PCM starts to cool down and release heat, first as sensible heat in liquid PCM, then as latent heat of fusion during the phase change, and finally as sensible heat in solid PCM until it reaches the temperature of the end walls.

Due to the non-linear, unsteady nature of the problem several assumptions were also made in this case to simplify the two-dimensional heat transfer problem. The assumptions were the following:

- initially the PCM is in a liquid state. The effect of natural convection is assumed to be negligible. The sole heat transfer mode is assumed to be conduction;
- the solidification temperature (T_m) is assumed to be constant;
- the temperature distribution of the fin is considered to be one-dimensional and to take place in the x-direction;
- in Region 1, heat transfer is one-dimensional and takes place only in the x-direction. The fin does not affect heat transfer in this region;
- in Region 2, the solid-liquid interface moves only one-dimensionally, in the y-direction, because the heat is mainly transferred through the fin to the environment;
- when the thermal diffusivity of the PCM α approaches zero ($\alpha = \frac{k}{\rho c_p} \approx 0$) it can be assumed that $\frac{\partial T}{\partial t} = 0$ and $T(x,t)=T_i$ in liquid PCM .The sensible heat of the liquid PCM is taken into account in the enhanced latent heat term $-\left[L + c_l(T_i - T_m)\right]$, which slows down the freezing front (Alexiades et al. 1993). Thus, the initial temperature of the PCM is the solidification temperature T_m rather than the initial temperature T_i.

The enhanced latent heat term slows down the freezing front, which starts to move directly when $t>0$ s, and

- in this approximation model the solidification process is assumed to start immediately when the walls are exposed to a lower temperature. The initial temperature of the fin is assumed to be T_m rather than T_i. Therefore, the derived analytical model is limited to use for short, highly conductive fins in which the temperature decreases quickly from the initial temperature to the solidification temperature.

In Region 1 the solidification can be handled as a one-dimensional one-phase Stefan problem, as in Paper IV. However, the cooling of the PCM before the solidification process is taken into account in the enhanced latent heat term $-\left[L + c_l(T_i - T_m)\right]$. The heat equation for a solid phase change material and for a solid-liquid interface with initial and boundary conditions can be written as:

$$\frac{\partial T_s}{\partial t} = \frac{1}{\alpha_s}\frac{\partial^2 T_s}{\partial x^2}, \qquad ,t>0 \qquad (64)$$

$$-\rho_s\left[L + c_l(T_i - T_m)\right]\frac{\partial S_x}{\partial t} = -k_s\frac{\partial T_s(S_x,t)}{\partial x} \qquad ,t>0 \qquad (65)$$

$$S_x(0)=0 \qquad (66)$$

$$T_s(S_x,t)=T_m \qquad (67)$$

$$T_s(0,t)= T_s(l_f,t)= T_w \qquad (68)$$

In Region 2, the energy balance for the fin can be rewritten with the initial and boundary conditions as:

$$\left(\rho c_p\right)_f D\frac{\partial T_f}{\partial t} = k_f D\frac{\partial^2 T_f}{\partial x^2} - \frac{k_s}{S_y}(T_f - T_m) \qquad ,t>0 \qquad (69)$$

$$T_f(x,0)=T_m \qquad (70)$$

$$T_f(0,t)= T_f(l_f,t)= T_w \qquad (71)$$

The heat equation for the phase change material and heat balance for the solid-liquid interface with initial and boundary conditions can be written as:

$$\frac{\partial T_s}{\partial t} = \frac{1}{\alpha_s}\frac{\partial^2 T_s}{\partial y^2}, \qquad ,t>0 \qquad (72)$$

$$-\rho_s\left[L + c_l(T_i - T_m)\right]\frac{\partial S_y}{\partial t} = -k_s\frac{\partial T_s(S_y,t)}{\partial y} \qquad ,t>0 \qquad (73)$$

$S_y(0)=0$ (74)

$T_s(S_y,t)=T_m$ (75)

To make possible the solution of Eqs. (69)-(71) the following dimensionless variables are introduced:

$$\theta = T_f - T_m, \quad \nu = \frac{k_s}{S_y(\rho c_p)_f D} \text{ and } \quad \kappa = \frac{k_s}{(\rho c_p)_f}.$$

Eqs. (69)-(71) can be rewritten using the dimensionless variables.

$$\frac{\partial \theta}{\partial t} = \kappa \frac{\partial^2 \theta}{\partial x^2} - \nu\theta \qquad ,t>0 \qquad (76)$$

$\theta(\eta,0) = 0$ (77)

$\theta(0,\tau) = \theta(1,\tau) = 1$ (78)

Eqs. (64)-(68), Eqs. (69)-(71 and Eqs.(76)-(78) are solved mathematically.

5.2 Solution

In Region 1, Eqs. (64)-(68) are solved with the quasistationary approximation method, which overestimates the location of the solidification front (Alexiades et al 1993). However, the overestimation will compensate for the fact that the problem is being handled one-dimensionally instead of two-dimensionally. The heat is transferred much more slowly from the storage to the environment in a one-dimensional case than in a two-dimensional case. The method consists of replacing the heat conduction equation with a steady-state equation, $\frac{\partial^2 T}{\partial x^2} = 0$. The distance of the solid-liquid interface from the end wall is

$$S_x = \sqrt{\frac{2k_s(T_w - T_m)t}{-\rho(L + c_l(T_i - T_m))}} \qquad (79)$$

In Region 2, the solution for the dimensionless temperature of the fin is (Carslaw et al. 1959)

$$\theta = \frac{\cosh(x)\sqrt{\nu/\kappa})}{\cosh(l_f/2\sqrt{\nu/\kappa})} - \frac{4}{\pi e^{\nu t}} \sum_{n=0}^{\infty} \frac{(-1)^n e^{-\kappa(2n+1)^2\pi^2 t/(2l_f)}}{(2n+1)\left[1 + \left\{\nu l_f^2/((2n+1)^2\pi^2\kappa)\right\}\right]} \cos((2n+1)\pi x/l_f) \qquad (80)$$

$$T_f = T_m + \theta(T_W - T_m). \tag{81}$$

Eqs. (72)-(75) are also solved with the quasistationary approximation method. The distance of the solid-liquid interface from the fin is

$$S_y = \sqrt{\frac{2k_s(T_f - T_m)t}{-\rho(L + c_l(T_i - T_m))}}. \tag{82}$$

Finally, the temperature of the fin T_f and the distance of the solid-liquid interface from the constant temperature end walls S_x and from the fin S_y are solved from Eqs. (79)-(82).

5.3 Results and discussion

The temperature distribution of the fin and the location of the solid-liquid interface were calculated using the derived one-dimensional analytical method (Eqs. (79)-(82)) and with the two-dimensional numerical effective heat capacity method (Eqs. (15)-(19)). The results were compared with each other to find the accuracy and performance of the one-dimensional analytical approach and the solution.

Three test cases with different geometry were chosen. In the test cases the initial temperature of the storage was 40°C and the PCM was in a liquid state. The wall temperature was set at 10°C. The phase change material used was paraffin and the fin material aluminium. The peak solidification temperature of the PCM was 25°C.

The half thickness D of the fin had a constant value of 0.5 mm in all the test cases. Otherwise, the geometry of the storage varied between the different cases. The width-to-height ratio $\lambda=l_f/l_c$ was given the values 0.2 in Case 1, 3.0 in Case 2, and 5.0 in Case 3.

The temperatures of the fin calculated with analytical and numerical methods in Cases 1 and 3 are presented in Paper V (Figs. 4 and 6). In Fig. 17 the results in Case 2 are shown at times t=200 s and 400 s.

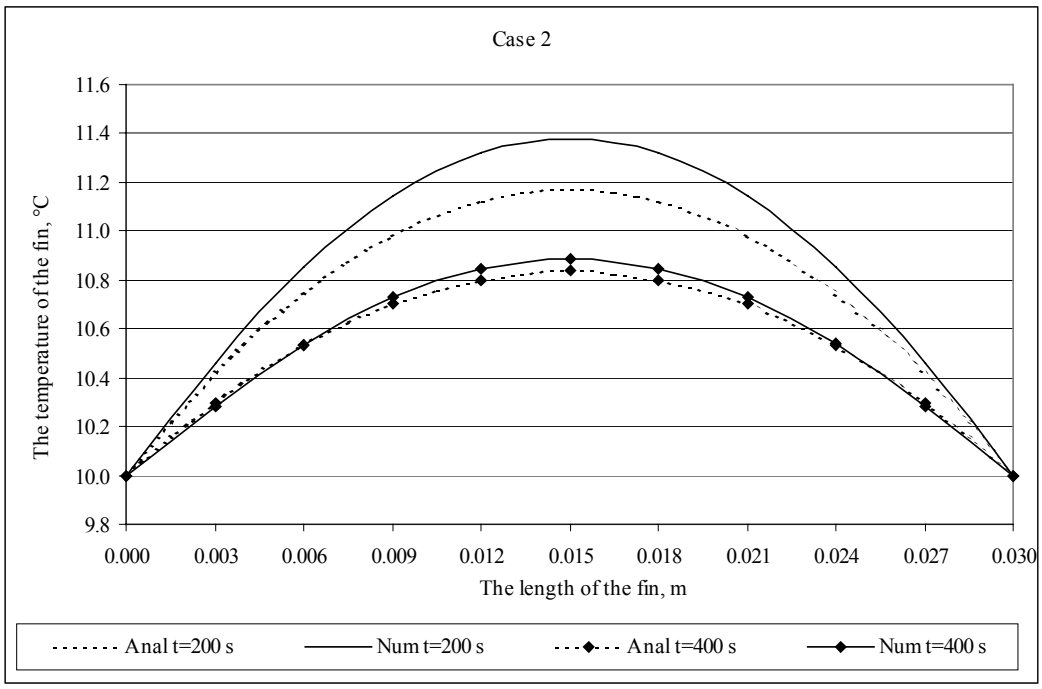

Figure 17. The temperature of the fin in PCM storage in Case 2 (λ=3, l_f=0.03 m, l_c=0.01 m).

At the beginning of the solidification process the temperature of the fin is lower in the analytical results than in the numerical results. The temperature difference between the analytical and numerical results is greatest in the case where λ =5.0. The reason for this phenomenon is the assumption that the fin was initially at the PCM's solidification temperature. As times increases, the difference in fin temperature between the analytical and numerical results diminishes. When the fin is short it achieves the end wall temperatures quickly because of its better heat conductivity compared to the conductivity of the phase change material. In that case the difference between the analytical and numerical results is small. Overall, the analytical model gives a satisfactory result for the temperature of the fin in all geometries.

The solid-liquid interface in different cases was calculated analytically and numerically. The location of the solid-liquid interface was defined from the temperature distribution of the storage, calculated using the effective heat capacity method by assuming that the interface is located at the temperature T_m=25°C.

In Fig. 18 the location of the solid-liquid interface in Case 2, calculated using the analytical and numerical methods at t=200 s and t=400 s, is presented. The results of Cases 1 and 3 are presented in Paper V (Figs. (7) and (9)).

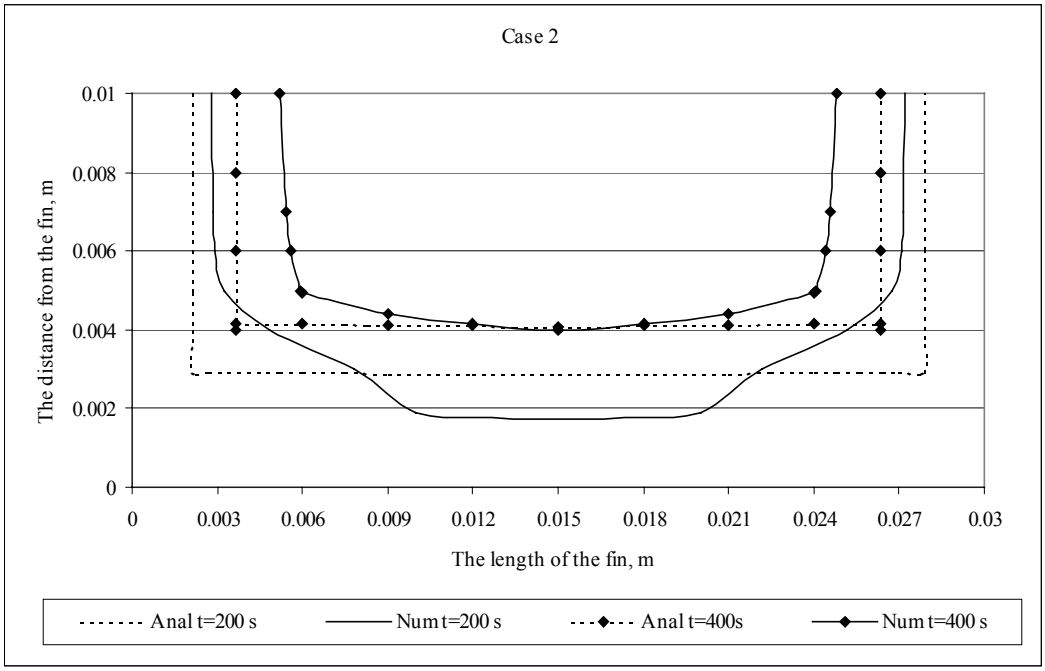

Figure 18. The location of the solid-liquid interface in analytical and numerical solutions in Case 2 (λ=3.0, l_f=0.03 m, l_c=0.01 m).

The derived analytical model is one-dimensional in both the x- and the y-directions. In reality the two-dimensional heat transfer in the storage accelerates the solidification process. It is also possible to see this phenomenon in Fig. 18. The interface in the one-dimensional analytical results moves more slowly than in the two-dimensional numerical results. However, the quasistationary solution compensates to a degree for the lack of two-dimensional heat transfer in the derived analytical method.

The numerical solution gives a rounder shape to the interface than the analytical solution because of the two-dimensional heat transfer effect in the numerical model. When the fin length increases, the assumption that the fin is initially at a lower temperature than the PCM starts to affect the results. However, the analytical solution still gives a satisfactory estimate of the solid-liquid interface location.

The fractions of solidified PCM (Eq. (63)) calculated from the derived analytical and numerical results in different test cases are shown in Table 5.

Table 5. The fraction of solidified PCM in different test cases.

	Time, s	Rate analytical, ε_{anal} -	Rate numerical, ε_{num} -	Error $\varepsilon_{anal}/\varepsilon_{num*100}$ %
Case 1. $\lambda=l_f/l_c$=0.2	200	0.61	0.55	5.8
	400	0.86	0.95	-9.1
Case 2. $\lambda=l_f/l_c$=3	200	0.44	0.39	5.1
	400	0.74	0.64	-5.1
Case 3. $\lambda=l_f/l_c$=5	300	0.45	0.38	7.3
	900	0.73	0.76	-3.3

The error made in the fraction of solidified PCM when using a derived one-dimensional analytical solution instead of a two-dimensional numerical solution was approximately ±10%. In the analytical model it is assumed that solidification begins directly when t>0 s. The sensible heat was taken into account in the enhanced latent heat term. Thus, it is obvious that the analytical model overestimated the solidification speed at the beginning of the solidification process. Later, when the time increases, the assumption that the analytical model is one-dimensional starts to affect the solidification speed and lowers it, while two-dimensional heat transfer accelerates the speed of solidification in the storage. Nevertheless, the derived analytical model gives a good estimate of the solidification of the PCM storage and the model can be used when the geometry of the storage is being studied in order to find the most effective geometry for a PCM storage with internal fins.

The assumptions that the fin is initially at the solidification temperature and that Eqs. (76)-(78) are valid when the solid-liquid interface location S_y is larger than zero mean that the model is limited to use with pre-defined maximum fin lengths. To find out the effect of the assumption, a numerical calculation using the effective heat capacity method is carried out with a geometry in which λ is given values from 0.2 to 8.0. The results show that with small λ values (λ =0.3 - 3.0) the cooling of the fin from the initial temperature to the solidification temperature happens quickly. The cooling time is less than 3 seconds. When λ increases, the cooling time increases exponentially. When λ=6.0 and the length of the fin is 0.06 m, the cooling time from the initial temperature to the solidification temperature of the PCM is 21 seconds. It was also noticed that when λ=6.0 and the length of the fin is 0.06 m, the term of the solid-liquid interface S_y approaches a value of zero at t=1 s. The conclusion was that the analytical model is valid when λ<6.0 and the length of the fin is l_f<0.06 m. In that case the effect of the assumption that the fin was initially at the solidification temperature of the PCM on the results was small and Eqs. (64)-(78) were solvable.

6 CONCLUSIONS

In this work heat transfer in the melting and solidification processes in finned PCM storages was studied analytically, numerically, and experimentally.

Different numerical methods were evaluated in order to find a straightforward and reliable numerical method for quick parametric studies and the comparison of several PCM storage alternatives. The numerical methods studied were the enthalpy method and the effective heat capacity method. The numerical predictions calculated with the FEMLAB multiphysics simulation tool were compared to experimental data. Both numerical methods gave good estimates of the temperature distribution of the storage during the melting and freezing processes. However, the effective heat capacity method with a narrow temperature range, dT=2°C, was the most precise numerical method when numerical results were compared to experimental results. It seemed that FEMLAB was very suitable for solving different kinds of phase change problems in one, two, or three dimensions.

The feasibility of using an infra-red (IR) camera to perform fast, quantitative visualisation of the interface during the experimental work was investigated. The temperature difference between the results achieved with the IR camera and thermocouples mounted inside the storage was approximately one degree, due to an internal calibration error in the camera. Although in this study thermocouples provided more reliable results than the IR camera, the feasibility of infrared thermography and its capacity for quantitative visualisation using infrared windows was confirmed.

A simplified analytical model based on a linear, transient, thin-fin equation which predicted the solid-liquid interface location and temperature distribution of the fin in the melting process with a constant imposed end wall temperature was presented. The two-dimensional heat transfer problem was simplified into a one-dimensional problem. The PCM storage was initially at the melting temperature of the PCM. The analytical results were compared to the numerical results and they showed good agreement. Due to the assumptions made in the model, the speed of the solid-liquid interface during the melting process was slightly too slow.

The work was extended to cover the solidification process in a finite PCM storage with internal fins with two different initial conditions: the storage was initially at the same temperature as, or a higher temperature than, the solidification temperature of the PCM. The analytical results were compared to the numerical results. A factor, called the fraction of solidified PCM, was also introduced. It was noticed that the assumptions made in simplifying the two-dimensional heat transfer problem into a one-dimensional form affected the accuracy to a greater extent than the assumptions made when solving the one-dimensional equations analytically. By using a one-dimensional approach instead of a two-dimensional approach, the accuracy was slightly reduced. However, the results were still satisfactory. The error made in the fraction of solidified PCM was smaller than ±10%, when the analytical model rather than the two-dimensional

numerical model was used. All in all, the accuracy of the approximate analytical model was satisfactory. The analytical models are useful in the pre-design stage of the storage. With the model it is possible to compare several storage alternatives in a reasonable time without the need to perform complicated numerical calculations.

7 REFERENCES

Alexiades V, Solomon A.D, Mathematical modelling of melting and freezing processes, Hemisphere Publishing Corporation, USA, 1993.

Al-Jandal S**,** Experimental study of temperature dependent heat transfer during melting and solidification processes. 2nd World Renewable Energy Congress, Reading University, U.K. 13-18 September, pp. 1097-1105, 1992.

Bonacina C, Comini G, Fasano A, Primicerio M, Numerical solution of phase-change problems. International Journal of Heat and Mass Transfer, Vol. 16, pp.1825-1832, 1983.

Bujage I, Enhancing thermal response of latent heat storage systems. International Journal of Energy Research, Vol 21, pp.759-766, 1977.

Carslaw H, Jaeger J, Conduction of Heat in Solids. 2nd Ed, Oxford University Press, New York, 1959.

Comsol AB, FEMLAB Version 2.3. Reference manual, 2002.

Crank J, Free and moving boundary problems. Oxford University Press, 1984.

Eftekhar J, Haji-Sheikh A, Lou D, Heat transfer enhancement in a paraffin wax thermal energy storage system. Journal of Solar Energy Engineering, Vol. 106, pp. 299-306, 1984.

Guenther R, Lee J, Partial differential equations and mathematical physics and integral equations. Dover Publications, Inc, 1988.

Henze R, Humphrey J, Enhanced heat conduction in phase-change thermal energy storage devices. International Journal of Heat and Mass transfer, Vol.24, pp.450-474, 1981.

Humphries W, Griggs E, A design handbook for phase change thermal control and energy storage devices. NASA TP-1074, 1977.

Incropera F, De Witt D, Fundamentals of heat and mass transfer. 3rd edition., John Wiley & Sons, New York, 1990.

Kroeger P.G, Ostrach S, The solution of a two-dimensional freezing problem including convection effects in the liquid region. International Journal of Heat and Mass Transfer, Vol. 17, pp. 1191-1207, 1973.

Lane G, Solar heat storage: Latent heat material. Vol 1, CRC Press, 1983.

Marshall R. Experimental determination of heat transfer coefficient in a thermal storage containing a phase change material - The rectangular cavity. International Conference on Future Energy Concept, pp. 216-220, 1979.

Marshall R. Natural convection effects in rectangular enclosures containing phase change material, Thermal heat transfer in solar energy systems, Kreith F; Boehm R;Mitchell J; Bannerot R.ASME pp.61-69, 1978.

Mehling H, Hiebler S, Ziegler F, Latent heat storage using a PCM-graphite composite material. Terrastock 8th International Conference on Thermal Energy Storage. August 28-September 1, Proceedings Vol. 1, pp. 375-380, 2000.

Padmahabhan P.V, Murthy M.V, Outward phase change in a cylindrical annulus with axial fins on the inner tube. International Journal Heat and Mass Transfer, Vol.29, No.12, pp.1855-1868, 1986.

Pal D Joshi Y Melting in a side-heated enclosure by uniformly dissipating heat source. International Journal of Heat and Mass Transfer, Vol. 44, pp. 375-387, 2001.

Peippo K. Basic thermodynamics mechanism of the phase change material storage and energy solutions. Department of Physics, Report TKK-F-B125, (in Finnish). 1989.

Peippo K, Kauranen P Lund P, A multicomponent PCM wall optimized for passive solar heating. Energy and Buildings, Vol.17, pp.265, 1991.

Stritih U, Novak P, Heat transfer enhancement at phase change processes. Terrastock 8th International Conference on Thermal Energy Storage. August 28-September 1, Proceedings Vol. 1, pp.333-338, 2000.

Velraj R et al. Heat transfer enhancement in a latent heat storage system. Solar Energy, Vol. 65, No.3. pp.171-180,1999.

Velraj R, Seeniraj R Hafner B, Experimental analysis and numerical modelling of inward solidification on a finned vertical tube for a latent heat storage unit. Solar Energy. Vol. 60. No.5. pp. 281-290, 1997.

Zivkivic B, Fujii I, An analysis of isothermal phase change of phase change material within rectangular cylindrical containers. Solar Energy, Vol.70, No.1, pp.51-61, 2001.

ORIGINAL PUBLICATIONS

I. Numerical and experimental investigation of melting and freezing processes in phase change material storage.

II. Validating a numerical phase change model by using infrared thermography.

III. Analytical model for melting in a semi-infinite PCM storage with an internal fin.

IV. Approximate analytical model for solidification in a finite PCM storage with internal fins.

V. Approximate analytical model for two-phase solidification problem in a finned phase change material storage.